BMJ Open

Protection levels of N95-level respirator solutions for the COVID-19 pandemic: safety concerns and quantitative evaluation procedures

Journal:	*BMJ Open*
Manuscript ID	bmjopen-2020-045557
Article Type:	Original research
Date Submitted by the Author:	06-Oct-2020
Complete List of Authors:	Ballard, David; Washington University in St Louis School of Medicine Mallinckrodt Institute of Radiology, Dang, Audrey ; Washington University in St Louis Kumfer, Benjamin ; Washington University in St Louis Weisensee, Patricia; Washington University in St Louis Meacham, J; Washington University in St Louis Scott, Alex; Washington University in St Louis Ruppert-Stroescu, Mary; Washington University in St Louis Burke, Broc; Washington University in St Louis Morris, Jason; Washington University in St Louis Gan, Connie; Washington University in St Louis Hu, Jesse; Washington University in St Louis King, Bradley; Washington University in St Louis Jammalamadaka, Udayabhanu; Washington University in St Louis Sayood, Sena; Washington University in St Louis Liang, Stephen; Washington University in St Louis Choudhary, Shruti; Washington University in St Louis Dhanraj, David ; Washington University in St Louis Maranhao, Bruno; Washington University in St Louis Millar, Christine; Washington University in St Louis Bertroche, J; Washington University in St Louis Shomer, Nirah; Washington University in St Louis Woodard, Pamela; Washington University in St Louis School of Medicine Mallinckrodt Institute of Radiology Biswas, Pratim; Washington University in St Louis Axelbaum, Richard; Washington University in St Louis Genin, Guy; Washington University in St Louis Williams, Brent; Washington University in St Louis Meacham, Kathleen; Washington University in St Louis
Keywords:	COVID-19, OCCUPATIONAL & INDUSTRIAL MEDICINE, Health & safety < HEALTH SERVICES ADMINISTRATION & MANAGEMENT, PREVENTIVE MEDICINE, Adult anaesthesia < ANAESTHETICS

Protection levels of N95-level respirator solutions for the COVID-19 pandemic: safety concerns and quantitative evaluation procedures

David H. Ballard, MD[1]; Audrey J. Dang BE[2]; Benjamin M. Kumfer, DSc[2]; Patricia B. Weisensee, PhD[3]; J. Mark Meacham PhD[3]; Alexander R Scott, BA, BS[4]; Mary Ruppert-Stroescu, PhD[5] Broc A. Burke, MD, PhD[6]; Jason A. Morris, BS[4]; Connie Gan, BS[4]; Jesse Hu, BS[4]; Bradley King[7]; Udayabhanu Jammalamadaka, PhD[1]; Sena Sayood, MD[8]; Stephen Y. Liang, MD[8]; Shruti Choudhary, BS[2]; David I A, Dhanraj, BS[2]; Bruno Maranhao, MD, PhD[6]; Christine Millar, MD[9]; J. Tyler Bertroche, MD[10]; Nirah H Shomer, DVM, PhD, DACLAM[11]; Pamela K Woodard, MD[1]; Pratim Biswas, PhD[2]; Richard L. Axelbaum, PhD[2]; Guy M. Genin, PhD[3,12,13]; Brent J. Williams, PhD[2]; Kathleen W. Meacham, MD, PhD[6]

1- *Mallinckrodt Institute of Radiology, Washington University School of Medicine, St. Louis, MO*
2- *Department of Energy, Environmental and Chemical Engineering, Washington University in St Louis, St. Louis, MO*
3- *Department of Mechanical Engineering & Materials Science, Washington University in St. Louis, MO*
4- *Washington University School of Medicine, St. Louis, MO*
5- *Sam Fox School of Design and Visual Arts, Washington University in St. Louis, St Louis, MO*
6- *Department of Anesthesiology, Washington University School of Medicine, St Louis, MO*
7- *Department of Environmental Health & Safety, Washington University School of Medicine, St. Louis, MO*
8- *Division of Infectious Diseases, Washington University School of Medicine, St. Louis, MO*
9- *Memorial Hospital Belleville; Belleville, IL*
10- *Department of Otolaryngology-Head & Neck Surgery, Washington University School of Medicine, St Louis, MO*
11- *Division of Comparative Medicine, Washington University School of Medicine, St. Louis, MO*
12- *NSF Science and Technology Center for Engineering Mechanobiology, Washington University in St. Louis, St Louis, MO*
13- *Bioinspired Engineering and Biomechanics Center, School of Life Sciences and Technology, Xi'an Jiaotong University, China*

Correspondence to:

Brent Williams, PhD
Raymond R. Tucker Distinguished InCEES Career Development Associate Professor
Director, Atmospheric Chemistry and Technology Lab
Dept. of Energy, Environmental & Chemical Engr.
Washington University
St. Louis, Missouri, 63110
Email: brentw@wustl.edu
Phone: (314) 935-9279

Kathleen W. Meacham, MD PhD
Assistant Professor
Department of Anesthesiology
Washington University School of Medicine
660 South Euclid Ave, Campus Box 8054
St. Louis, Missouri, 63110
Email: meachamk@wustl.edu
Phone: (314) 393-4117; Fax: (314) 362-8334

Twitter handles: DHB (@DavidBallardMD), PKW (@PamelaWoodardp), PB (lab) (@AAQRL_Biswas)

Short title: Safety of public N95 respirator solutions

Funding and Disclosures: All authors - No relevant disclosures related to the present study. No study-specific funding. BAB and KWM receive salary support from International Anesthesiology Research Society Mentored Research Award. AJD was supported by a National Science Foundation Graduate Research Fellowship (DGE-1745038). Any opinions, findings, and conclusions or recommendations expressed in this material are those of the authors and do not necessarily reflect the views of the National Science Foundation.

Acknowledgements: The Washington University N95 design task force for their support and facilitating testing.

Manuscript Type: Original/Laboratory Investigation; Abstract Word Count: 290; Manuscript Word Count: 3,723; Numbers of Figures: 5; Supplemental Figure: 3; Supplemental Documents: 1 Supplemental Document with 2 Supplemental Figures and 1 Table

Keywords: COVID-19; N95 respirator; personal protective equipment; filtering facepiece respirator; 3D printing

Protection levels of N95-level respirator solutions for the COVID-19 pandemic: safety concerns and quantitative evaluation procedures

ABSTRACT

Objective: The COVID-19 pandemic has precipitated widespread shortages of filtering face-piece respirators (FFRs) and the creation and sharing of improvised solutions (novel designs, repurposed materials) with limited testing against regulatory standards. We aimed to categorically test the efficacy and fit of improvised N95 respirator solutions using protocols that can be replicated in university laboratories.

Setting: Academic medical center with occupational health-supervised fit testing along with laboratory studies.

Participants: Adult volunteers with who passed quantitative fit testing for small and regular size commercial N95 respirators.

Methods: Five open-source N95 solutions were evaluated and compared to commercial National Institute for Occupational Safety and Health (NIOSH)-approved N95 respirators as controls. Fit testing using the 7-minute standardized Occupational Safety and Health Administration (OSHA) fit test was performed. In addition, protocols that can be performed in university laboratories for materials testing (filtration efficiency, air resistance, and fluid resistance) were developed to evaluate alternate filtration materials.

Results: Among five open-source, improvised solutions evaluated in this study, only one (which included a commercial elastomeric mask and commercial HEPA filter) passed a standard quantitative fit test. The four alternative materials evaluated for filtration efficiency (67% to

89%) failed to meet the 95% threshold at a face velocity (7.6 cm/s) equivalent to that of a NIOSH particle filtration test for the control N95 FFR. In addition, for all but one material, the small surface area of two 3D-printed solutions resulted in air resistance that was above the maximum in the NIOSH standard.

Conclusions: Testing protocols such as those described here are essential to evaluate proposed improvised respiratory protection solutions, and our testing platform could be replicated by teams with similar cross-disciplinary research capacity. Healthcare professionals should be cautious of claims associated with improvised respirators when suggested as FFR substitutes.

STRENGTHS AND LIMITATIONS

-Manufacturing of open source N95 solutions, quantitative fit testing, filtration testing, and material testing reflecting a method for others in a university lab setting to test N95 solutions for a pandemic-related response

-Quantitative fit testing according to Occupational Safety and Health Administration provides an objective measure of how the N95 alternative solutions perform on individuals that passed fit testing on commercial N95 respirators

-Filtration data gives performance of improvised filter materials and how they perform at velocities relevant to normal breathing and filtering in the range of SARS-CoV-2 viral particles

-Limitation of the production of these open source solutions were produced to the best of the author's understanding of posted instructions and did not attempt improvised solutions to improve the mask designs

INTRODUCTION

Personal protective equipment (PPE) is critical for limiting infectious disease risk to clinicians. During the Coronavirus Disease 2019 (COVID-19) pandemic, the World Health Organization noted in February 2020 that the global stockpile of PPE was insufficient, particularly for masks and filtering facepiece respirators (FFRs).[1] In a survey in March 2020 by the Association for Professionals in Infection Control and Epidemiology, nearly half of respondents reported that their healthcare facility's N95 FFR supply was nearly or completely depleted.[2] To address these shortages, many institutions developed alternatives to commercial filtering facepiece (FFR) respirators to provide immediate stopgap solutions.[2-11] Some of these alternative solutions were publicly disseminated, often with limited testing of key attributes including filtration, breathability, fit, and liquid fluid repellency.

Key functional attributes of N95 FFRs

In the United States, surgical N95 FFRs used by healthcare personnel are regulated by both the National Institute for Occupational Safety and Health (NIOSH) and the Food and Drug Administration (FDA). The surgical N95 respirator serves to protect wearers by filtering fine particles, providing a tight seal around the face, and repelling fluid splatter, while ensuring ease of breathing (**Figure 1**).[12, 13] Particle filtration efficiency is dependent on the size of the particle, the material properties of the respirator, and the face velocity at which the particle approaches the material; the face velocity depends on the user's instantaneous respiratory rate and the shape and size of the respirator itself. Respirator form must ensure that all breathed air passes through the filtration medium and does not leak from an edge. Lower flow resistance (larger surface area, material with lower pressure drop) reduces the work of breathing, mitigating wearer fatigue. The respirator must be comfortable, and respirator materials cannot pose health risks to the wearer (i.e., should not shed hazardous particles or fibers that can be inhaled). During crises, the respirator may need to function over periods of extended use and be reused; therefore, the respirator should be suitable for sterilization and maintain structural integrity. Finally, in the patient care environment, the filter material and/or an outer covering should repel high-velocity fluid splatter.

Due to the critical shortage of N95 respirators, many institutions have resorted to using locally improvised masks which have not undergone appropriate safety testing. As such, a discrepancy may exist between the respiratory protection actually provided by an improvised design and that the level of protection which healthcare workers would expect of a commercial respirator. Testing recently developed, open source designs intended as substitutes for N95 respirators, we present our framework of establishing an institutional platform for evaluating these improvised designs and materials, including fit, filtration, and fluid repellancy testing. This framework could be replicated by collaborative teams with similar cross-disciplinary expertise and laboratory capabilities.

METHODS

Overview

Our Institutional Review Board determined that this study (which included fit testing of respirator designs by adult volunteers without collection of personal data) was designated nonhuman subjects research. Five respirator designs that have been publicly circulated as N95 solutions were evaluated to demonstrate testing procedures and identify efficacy and potential limitations (**Figure 2**): a cloth-based respirator ("Sewn Sterilization Wrap")[7], three 3-D printed respirators ("P100 Adaptor"[8], "Self-Moldable 3D Printed"[9], and "Multi-Part 3D Printed"[10]), and one repurposed from medical supplies ("Elastomeric")[11]. These were produced as detailed in **Supplemental Document**. A commercial NIOSH-approved N95 respirator (disposable 3M 1860 Health Care Particulate N95 FFR Respirators, 3M, St. Paul, MN) served as control. Experiments were performed in laboratories at our institution. Testing included OSHA-standard quantitative fit testing, filtration testing in an aerosols laboratory, and liquid repellancy testing in a surface chemistry laboratory.

Filtration efficiency and liquid repellancy were evaluated for Halyard H600 sterilization wrap (O&M Halyard, Inc., Alpharetta, GA, USA) and Filti™ Face Mask Material (Filti, Inc., Lenexa, KS, USA). In addition, filtration efficiency was also evaluated for a second Halyard sterilization wrap (H500), material from a commercial N95 respirator (3M™ VFlex™ Healthcare Particulate Respirator and Surgical Mask 1804, 3M, St Paul, MN), and commercial HVAC material (MERV16 rating), and other configurations of the sterilization wrap materials (two layers of H600, single layers of H600 with stitching).

Patient and public involvement

No patients were involved.

Quantitative respiratory fit testing

Respirators were quantitatively tested via OSHA 7-minute standardized fit test[14] using a PortaCount Respirator Fit Tester Model 8048 and TSI Model 8026 Particle Generator with TSI

FitPro Ultra software. A 4 mm metal grommet was punched through each respirator at a location not in direct contact with skin and connected with 4 mm tubing to the PortaCount device. To facilitate testing of 3D printed respirators, the grommet was inserted through the filter material. To permit passage of a grommet into the filter of the Multi-Part 3D Printed respirator, a soldering iron was used to create a hole in the thermoplastic cap overlying filtration material Three adult volunteers served as standard faces (2 regular, 1 small). The Self-Moldable 3D Printed respirator was molded using hot water as described in design instructions (**Supplemental Document**). Each user adjusted respirator placement and strap tightness during real-time fit testing to achieve the best possible fit prior to the 7-minute OSHA standard test. Each design was tested on faces calibrated to small and regular sized surgical N95 filtering facepiece respirators.

Filtration and breathability testing

Particle filtration performance was evaluated for several materials including commercial filtration materials and fabrics intended for other medical uses. Additional information about testing procedures and a sampling diagram can be found in **Supplemental Document**. Sample discs of 47 mm were cut directly from the mask or the sourced material sheet and placed in an in-line filter holder during filtration testing. A polydisperse NaCl aerosol was produced using a Collison nebulizer, dried to remove water content, and then passed through a charge neutralizer and an electrostatic classifier (TSI Inc., Model 3080 with long differential mobility analyzer column), which selected particles based on their mobility in the electric field with a single-charge diameter setpoint of 300 nm (**Supplemental Document** for additional discussion of the particle size). The size-classified aerosol was then charge-neutralized a second time and diluted using HEPA-filtered air to achieve a final particle number concentration in the range of 3000-4000 #/cc. As per our intention to evaluate how these improvised designs compare to the N95 respirators in short supply, this selected size is consistent with similar filtration studies of N95 respirators.[15] Though this diameter is somewhat larger than the size of an isolated SARS-CoV-2 viral particle (approximately 75-105 nm), the virus would most likely be in a larger respiratory particle consisting primarily of water, proteins, salts, and surfactants.[16, 17]

To determine filtration efficiency, particle concentrations upstream and downstream of the filter were measured via continuous condensation particle counter (TSI Inc., Model 3022A). Concentrations were measured in immediate succession to mitigate impact of drift in nebulizer output over time. The NIOSH N95 protocol demands a flow of 85 LPM through the entire respirator, reported to yield a face velocity in the range of 10-13 cm/s for surface areas typical of commercial N95 respirators.[18] We report results here for tests at 7.6 ± 0.1 cm/s, based on the calculated face velocity for the N95 FFR in this study. Particle filtration efficiency values reported here are the average of the three to four different filter punches for the same material, Methods for these calculations are included in **Supplemental Document**. The pressure drop across the filter material along with the temperature and relative humidity of the gas passed through the filter were recorded.

Liquid repellency and splatter testing

Liquid repellency of two of the fabrics used in the alternative respirator designs, Halyard H600 and Filti, were tested through contact angle and fluid penetration measurements. Advancing and receding contact angles were measured by slowly increasing and decreasing the volume of a sessile droplet using a 30 gauge needle and analyzed using ImageJ. [19] Textile liquid absorbency was evaluated via AATCC test method 79-2018.[20] Blood splatter testing followed ASTM F1862 ("Resistance of Medical Face Masks to Penetration by Synthetic Blood") procedures, with the following exceptions: i) Room-temperature whole milk, dyed with red food coloring, replaced the synthetic blood. The surface tension γ_l=49.7 ± 2.0 mN/m was determined using the pendant drop method with a 16 gauge needle, and was independent of the dye concentration.[21] ii) Fabrics were typically not pre-conditioned at 85% relative humidity (RH). Instead, most were stored in a regular laboratory environment (35-55% RH, 22 ± 1°C). iii) Only a limited number of tests (1 to 3 tests) were performed for each impact velocity and fabric. iv) Pressure levels to achieve the required liquid impact velocities (4.5, 5.5, and 6.35 m/s; experimental uncertainty of ± 0.07 m/s) were approximately 34, 50, and 65 kPa, respectively, and were calibrated prior to every test session.

RESULTS

Quantitative respirator fit testing

All but one improvised N95 solution evaluated failed to reach the OSHA half-mask respirator overall fit factor minimum of 100; only the Elastomeric solution (which uses a commercial HEPA filter for particle filtration mounted to a commercial anesthesia face mask) passed quantitative fit on both small and large face standardized users. Common points of fit failure between respirators were air leak around the nose and difficulty with strap tightening. For 3D printed respirators, users experienced discomfort due to respirator contact at the chin and bridge of the nose. Individual fit factors and points of failure are noted in **Figure 2** and **Supplemental Document.** Components of the quantitative fit test for each N95 solution is noted in **Figure 3.** The Sewn Sterilization Wrap solution failed to reach OSHA specifications (fit factor > 100) for both small and regular respirator size (overall fit factor 20 and 17 respectively. A poor seal was noted around the nose and chin and the rigidity of the straps complicated proper tightening. A fit test was not completed for the P100 filter respirator on small size standardized users due to grossly inadequate seal. Poor fit was additionally noted for regular size standardized users, overall fit factor 17. The Self-Moldable 3D-printed respirator additionally failed to meet OSHA fit standards, overall fit factors 11 and 12 respectively after heat molding. The overall fit factor for the Self-Moldable 3D-printed respirator was not improved by heat molding to users' faces, although it improved subjective user perception of fit with no subjectively noticeable air leak during normal breathing. The Multi-Part 3D printed respirator additionally achieved poor quality seal, overall fit factor 4 and 15 respectively. Users noted circumferential air leak as well as potential air leak surrounding the filter screw threads. The Elastomeric respirator passed fit testing for both small and regular size standardized users, overall fit factor 110 and 108 respectively, however the respirator had inconsistent performance across sections of the fit test and users noted discomfort with the weight of the filter, work of breathing, and strap tightness at which good fit was achieved.

Quantitative fit factors reflect infiltration of particles through both face seal leakage and material penetration, though typical N95 FFRs have such high average filtration efficiency that poor fit is the more likely cause of failed tests (**Supplementary Figure 1**). For improvised designs and materials, particle penetration through the filter media itself could contribute a larger fraction of particles which infiltrate the FFR, as these materials typically have poorer filtration performance. In addition, the 3D-printed designs have a lower filter media surface area, and the resulting higher air face velocities would decrease filtration performance.

Material filtration and air resistance testing

Only the commercial N95 mask material (3M™ VFlex™ Healthcare Particulate Respirator and Surgical Mask 1804, 3M, St Paul, MN) filtered more than 95% of 300 nm particles at a face velocity of 7.6 cm/s (**Figure 4**). In addition, the commercial N95 material had a modest pressure drop of 50 Pa (95% CI: 32 - 69) at this face velocity.

The quality factor (Q) enables evaluation of the trade-off between filter media filtration performance and pressure drop:

$$Q = \ln(1/(1-E)) / \Delta P$$

where E is filtration efficiency, and ΔP is pressure drop. The HVAC (MERV16) and Filti materials had higher quality factors than the sterilization wrap materials, though their performance was more variable (a range of 12% among four punches of Filti and 13% among three punches of the HVAC material). Two sterilization wrap materials (H500 and H600) were tested in a variety of arrangements. As a single layer, H500 and H600 performed similarly, with slightly higher filtration efficiency (70% (95% CI: 67%-72%)) and pressure drop (50 Pa (95% CI: 34 - 66)) for H600. A double layer of H600 (with the flat, less textured sides of the two layers facing inward) improved the filtration efficiency to 89% (95% CI: 86%-91%), though the pressure drop increased. The filtration efficiency measurement for two layers of H600 sterilization wrap was within 5% of that measured by Ou et al.[20], who also evaluated the impact of dry heat, steam, and alcohol decontamination cycles at additional particle diameters.

To evaluate the impact of stitching Halyard material, two lines of stitches (between 6.5 and 7.0 cm total length) were made with a sewing machine in the center of 47 mm discs of H600 material (**Supplemental Document**). The impact of stitching was a decrease in the filtration efficiency from the single layer H600 of 70% (95% CI: 67%-72%) to 65% (95% CI: 60%-71%) for the stitched H600, which also had more variable performance.

A summary of the filtration efficiency and pressure drop measurements are provided in **Supplemental Table 1**.

Supplemental Table 1.

	Filtration Efficiencies of Replicate Punches (%) (Standard Uncertainty)				Mean Filtration Efficiency (%)	Mean Pressure Drop (Pa)
	Punch #1	Punch #2	Punch #3	Punch #4	(95% Confidence Interval)	(95% Confidence Interval)
VFlex ™ (N95)	99.659% (99.649% - 99.669%)	99.67% (99.65% - 99.69%)	99.600% (99.590% - 99.610%)		99.64% (99.55% - 99.74%)	50 (32 - 69)
HVAC (MERV 16)	83.8% (83.3% - 84.3%)	79.7% (79.2% - 80.3%)	70.3% (69.5% - 71.1%)		78% (65% - 91%)	12 (3 - 22)
Filti™	81% (80% - 82%)	90.9% (90.7% - 91.2%)	93.2% (93.0% - 93.4%)	89.3% (89.0% - 89.6%)	89% (81% - 96%)	43 (31 - 55)
H600 (2 Layers)	87.5% (87.1% - 87.8%)	89.0% (88.7% - 89.3%)	89.7% (89.4% - 89.9%)		89% (86% - 91%)	124 (114 - 133)
H600 (1 Layer)	69.6% (68.8% - 70.4%)	70.7% (69.8% - 71.6%)	68.4% (67.6% - 69.2%)		70% (67% - 72%)	50 (34 - 66)
H600 Stitched	62% (60% - 63%)	65% (64% - 67%)	68.3% (67.4% - 69.2%)		65% (60% - 71%)	45 (35 - 54)
H500	66.9% (66.0% - 67.7%)	65.9% (64.9% - 66.9%)	68.4% (67.6% - 69.2%)		67% (65% - 69%)	40 (19 - 61)

Supplemental Table 1. Summary of filtration efficiency and pressure drop measurements

Breathability of improvised designs

At the test face velocity in this study (7.6 cm/s), none of the materials exceeded the maximum pressure drop across the filter in the NIOSH standard for N95 respirators (343 Pa H_2O during inhalation and 245 Pa during exhalation) to avoid discomfort and detrimental physiological effects.[18, 19] However, the actual face velocity of a respirator undergoing this test (at a flowrate of 85 L/min) would depend on the surface area of filtration material (**Supplemental Figure 2**). For fibrous filters, pressure drop and face velocity are proportional, such that we can use our measurements at a single face velocity to model the pressure drop of each material at the face velocity at which 85 L/min of air would flow through the surface area of each design[22] (**Supplemental Figure 3**).

For all materials, the modeled pressure drop of the Sewn Sterilization Wrap Mask is lower than the maximum standard for inhalation and exhalation. By contrast, only the HVAC material is modeled to meet this breathability standard for any of the 3D printed designs. If the closed area of the mesh grid of the Multi-Part 3D Printed mask is not counted as available filtration surface area, then not even the HVAC material is predicted to meet the NIOSH air resistance standard when used with this design.

Liquid repellency and splatter testing

Test results and optical images of the fabric surfaces (**Figure 5**) shows that both H600 and Filti are repellent towards deionized water and milk (part A: advancing contact angles ≥ 120°), but pose potential liquid penetration points due to millimetric holes in their design. For Halyard, these holes appear sealed, whereas for Filti, the composite fabric consists of a very thin continuous layer sandwiched between two outer layers with the holes in vertical alignment. Both fabrics passed the textile absorbency test with no visible liquid penetration even after multiple minutes. Furthermore, while receding contact angles of milk on both fabrics are zero, milk stains were easily removed by wiping the surface with a wet cloth. When subject to the high-velocity milk jet (part B), however, both fabrics failed splatter testing for a single layer, as confirmed by liquid penetration (part C, bottom image "Layer 1"). When used in a double-layer, H600 was able to prevent liquid break-through for all jet velocities, whereas Filti failed even as a double-layer at higher impingement velocities. Whereas liquid penetration for the top layer happened uniformly at the location of jet impact, penetration for the bottom layer appeared predominantly through the holes in the fabric, and hence was observed more commonly for Filti and not for H600.

DISCUSSION

The COVID-19 pandemic has created significant worldwide shortages in N95 filtering facepiece respirators[23-27] which necessitated development and publication of alternative mask solutions.[6-11] Given the urgency for these N95 solutions, safety and efficacy testing prior to their use was limited. Here we presented the results of rigorous, quantitative testing on some of the first open-source alternative N95 solutions created to address the critical N95 respirator shortage at the start of the COVID-19 pandemic. In this work, a collaborative, interdisciplinary team quantitatively evaluated fit, filtration, and material properties of these N95 open-source solutions.

Apart from the commercial N95 FFR, only the Elastomeric solution passed quantitative fit testing. This design leverages key attributes of its commercial components, including high quality fit of a commercial anesthesia mask and high filtration efficiency of HEPA filter. While we did not directly test the air resistance of a single HEPA filter, the manufacturer's specification (35 mm H2O at 60 L/min) indicates that it exceeds the NIOSH standard (25 mm H2O for exhalation) even at a flowrate (60 L/min) lower than that of the NIOSH test (85 L/min).[28] Thus, a bifurcated adapter for simultaneous use of two filters is recommended for adequate breathability (modeled as 24.8 mm H_2O at 85 L/min). Although the Elastomeric solution did pass, its basis off an existing commercial design may limit its implementation for mass production and distribution, as it depends on the availability of the product compared to the manufacturing capabilities of sewn masks or 3D printed designs.

The Sewn Sterilization Wrap Mask was well-tolerated by users, and its larger surface area results in a modeled pressure drop (for all materials) which among the improvised solutions is most similar to the commercial N95 FFR. Both material filtration testing and quantitative fit testing indicate that its respiratory protection is not equivalent to that of an N95 FFR, though it is likely superior to that of a surgical mask (**Supplementary Figure 1**). Two layers of sterilization wrap also demonstrated fluid resistance in a test with a high velocity jet of milk, though this was not strictly equivalent to the regulatory test method. Filti face mask material would not be an appropriate alternate material for improvised surgical masks or FFRs, unless combined with an additional layer that provided fluid resistance. We note that use in masks is an off-label application of sterilization wrap.

The 3D printed designs yielded 5 of the 6 poorest quantitative fit scores. Quantitative fit testing does not discriminate between particles which infiltrate through leaks in the face seal (or through defects) and particles which penetrate the filtration media itself. The rigidity of the 3D printed designs compromised fit (as well as comfort), and the limited surface area likely exacerbated penetration through the filtration media itself. Though some reports have suggested the use of individual-specific 3D printed masks based on their facial topography, although this may not be practical for a mass production standpoint.[29, 30] At the face velocity calculated for the N95 FFR in this study at the flowrate of a NIOSH particle filtration test, none of the alternate materials filtered more than 95% of particles.[19] Since their lower surface area would result in a higher face velocity in an NIOSH particle filtration test, the 3D printed masks would likely have lower filtration efficiency than reported here for these materials. Only the HVAC material was modeled to have low enough air resistance for the 3D printed designs at these high face velocities, such that we recommend pressure drop measurements of specific filter media proposed for these designs. More specifically, measuring or modeling air resistance at the face velocity which would be encountered in a NIOSH test (at 85 L/min) enables a direct comparison of an improvised design with the N95 standard.

Even without direct filtration testing of full prototypes (which is experimentally more demanding), we demonstrate how quantitative fit testing and material filtration testing can be combined to screen proposed improvised designs together with consideration of air and fluid resistance. These results point to a fundamental need to improve facial fit in future respirator designs, and even more acutely, to an ongoing need during this pandemic for end-users to be equipped and educated for some measure of fit testing. In addition, evaluating designs at the conditions of regulatory test methods (ex. appropriate face velocity for filtration and air resistance) enables direct comparison to the performance expected of a N95 FFR.

There are several limitations to the present study. The improvised respirator solutions were reproduced to the best understanding of posted instructions; however the tested designs may not reflect interval improvements. While filtration testing of material patches at relevant conditions can inform material selection for further development, filtration tests of a mask prototype in its complete form is necessary for evaluation against N95 NIOSH standards, and we continue to develop in-house capacity for these tests. A complication is that the face velocity of a mask depends upon a user's minute ventilation, respiratory rate, inspiratory time, and the mask surface area, complicating comparison of masks and protocol standardization. Whole milk was used to test the splatter resistance of the fabrics, as artificial blood was not readily accessible. While the measured surface tension is within the range of surface tension of typical body fluids and blood at body temperature [21, 31] it is slightly higher than that of synthetic blood as prescribed by F1862, which could result in favorable test results, as fluids with lower surface tension are known to wet surfaces more easily.[32]

The N95 respirator alternative solutions tested here were attempts to meet immediate needs of the COVID-19 pandemic frontline. However, our data indicates the majority of these solutions do not have equivalent respiratory protection and breathability to a N95 FFR. The majority of masks tested revealed inherent design issues such as inadequate filtration capabilities of the base materials and poor ergonomic facial fit to a variety of facial shapes and sizes. Our experience has highlighted the importance for institutions to be equipped and educated to perform appropriate qualitative and quantitative testing prior to novel mask implementation. This study reveals that rapid creation of an improvised respirator with N95 performance utilizing readily available materials and simple manufacturing methods is extremely challenging, and consequently there is an emergent need for in-house testing platforms to better understand the degree to which protection is being provided. Healthcare professionals requiring this a high level of respiratory protection should be cautious of claims associated with improvised respirators when suggested as N95 replacements without quantitative evaluation.

REFERENCES

1. Rational Use of Personal Protective Equipment for Coronavirus Disease 2019 (COVID-19) – Interim Guidance February 27, 2020. World Health Organization Website. Available at: https://apps.who.int/iris/bitstream/handle/10665/331215/WHO-2019-nCov-IPCPPE_use-2020.1-eng.pdf Accessed on October 2, 2020.
2. "Protecting Healthcare Workers During the COVID-19 Pandemic: A Survey of Infection Preventionists March 27, 2020." Association for Professionals in Infection Control and Epidemiology. Available at: https://apic.org/wp-content/uploads/2020/03/Protecting-Healthcare-Workers-Survey_Report_3_26_20_Final.pdf. Accessed on July 7, 2020.
3. Provenzano D, Rao YJ, Mitic K, Obaid SN et al. Rapid Prototyping of Reusable 3D-Printed N95 Equivalent Respirators at the George Washington University. *Biomedical and Chemical Engineering* 2020; 2020030444. Ahead of print. doi:10.20944/preprints202003.0444.v1
4. Liu DCY, Koo TH, Wong JKK, et al. Adapting re-usable elastomeric respirators to utilise anaesthesia circuit filters using a 3D-printed adaptor - a potential alternative to address N95 shortages during the COVID-19 pandemic. *Anaesthesia*. 2020;75(8):1022–1027.

5. Elkington P, Dickinson A, Mavrogordato M, et al. A Personal Respirator Specification for Health-care Workers Treating COVID-19 *(PeRSo)*. Ahead of print. doi:10.31224/osf.io/rvcs3.

6. COVID-19 Supply Chain Response Collection. NIH 3D Print Exchange Website. Available at: https://3dprint.nih.gov/collections/covid-19-response/search Accessed on October 2, 2020.

7. Mask Alternative. University of Florida College of Medicine Department of Anesthesiology Website. Available at: https://anest.ufl.edu/clinical-divisions/mask-alternative/#prototype2 Accessed on October 2, 2020.

8. 3D Printed N95 Replacement Mask. Barrow Neurological Institute Website. Available at: https://www.barrowneuro.org/get-to-know-barrow/barrow-innovation-center-2/3d-printed-n95-mask/. Accessed on October 2, 2020.

9. The Montana Mask. Make the Masks Website. Available at: https://www.makethemasks.com/. Accessed on October 2, 2020.

10. The "MalaMask" Project (N95 Alternative Filter). River City Labs Website. Available at: https://wiki.rivercitylabs.space/covid-19/3d-printed-masks. Accessed on October 2, 2020.

11. Surgical Innovation Fellowship. Boston Children's Hospital Website. Available at: http://www.childrenshospital.org/research/departments-divisions-programs/departments/surgery/surgical-innovation-fellowship. Accessed on October 2, 2020.

12. Radonovich LJ, Jr, Simberkoff MS, Bessesen MT, et al. N95 Respirators vs Medical Masks for Preventing Influenza Among Health Care Personnel: A Randomized Clinical Trial. *JAMA* 2019;322(9):824-33.

13. Janssen L, Ettinger H, Graham S, Shaffer R, Zhuang Z. The use of respirators to reduce inhalation of airborne biological agents. *J Occup Environ Hyg.* 2013;10:D97-D103.

14. Appendix A to §1910.134—Fit Testing Procedures (Mandatory). United States Department of Labor Website. Available at: https://www.osha.gov/laws-regs/regulations/standardnumber/1910/1910.134AppA. Accessed on October 2, 2020.

15. Balazy A, Toivola M, Reponen T, Podgorski A, Zimmer A, Grinshpun SA. Manikin-Based Performance Evaluation of N95 Filtering-Facepiece Respirators Challenged with Nanoparticles. *Ann Occup Hyg.* 2005;50:259-69.

16. Martines RB, Ritter JM, Matkovic E, et al. Pathology and Pathogenesis of SARS-CoV-2 Associated with Fatal Coronavirus Disease, United States. Emerging Infect Dis. 2020;26(9).

17. Johnson, G. R.; Morawska, L.; Ristovski, Z. D.; Hargreaves, M.; Mengersen, K.; Chao, C. Y. H.; Wan, M. P.; Li, Y.; Xie, X.; Katoshevski, D.; et al. Modality of Human Expired Aerosol Size Distributions. *J. Aerosol Sci.* **2011**, *42* (12), 839–851.

18. Airflow resistance test. Cornell Law School Legal Information Institute. Available at https://www.law.cornell.edu/cfr/text/42/84.172 Accessed on October 2, 2020.

19. Chen V, Long K, Woodburn EV. When weighing universal precautions, filtration efficiency is not universal. *J Hosp Infect*. 2020. Ahead of print. DOI: 10.1016/j.jhin.2020.04.032.

20. Ou Q, Pei C, Chan Kim S, Abell E, Pui DYH. Evaluation of decontamination methods for commercial and alternative respirator and mask materials – view from filtration aspect. J Aerosol Sci. 2020;150:105609.

21. Stalder AF, Kulik G, Sage D, Barbieri L, Hoffmann P. A snake-based approach to accurate determination of both contact points and contact angles. *Colloid Surface A.* 2006;286:92-103.

22. Hinds, W. C. *Aerosol Technology*, 2nd ed.; Wiley: Hoboken, 1999.

23. van Doremalen N, Bushmaker T, Morris DH, et al. Aerosol and Surface Stability of SARS-CoV-2 as Compared with SAS-CoV-1. *N Engl J Med* 2020;382:1564-7.

24. Bauchner H, Fontanarosa PB, Livingston EH. Conserving Supply of Personal Protective Equipment—A Call for Ideas. *JAMA* 2020;323(19):1911.

25. Wong SC-Y, Kwong RT-S, Wu TC, et al. Risk of nosocomial transmission of coronavirus disease 2019: an experience in a general ward setting in Hong Kong. *J Hospl Infect* 2020;105(2):119–127.

26. Lu J, Gu J, Li K, et al. COVID-19 Outbreak Associated with Air Conditioning in Restaurant, Guangzhou, China, 2020. *Emerg Infect Dis.* 2020;26.

27. Santarpia JL, Rivera DN, Herrera V, et al. Transmission Potential of SARS-CoV-2 in Viral Shedding Observed at the University of Nebraska Medical Center. *Infectious Diseases (except HIV/AIDS)* 2020. Ahead of print. doi:10.1101/2020.03.23.20039446.

28. Ultipor® 25 Anesthesia Filter with Monitoring Port . Available at: https://shop.pall.com/us/en/products/zidBB25AB?CategoryName=&CatalogID=&tracking=searchterm. Accessed October 2, 2020.

29. Swennen GRJ, Pottel L, Haers PE. Custom-made 3D-printed face masks in case of pandemic crisis situations with a lack of commercially available FFP2/3 masks. Int J Oral Maxillofac Surg. 2020;49(5):673–677.

30. Scott AR, Hu J, Gan C, Morris JA, Meacham KW, Ballard DH. Safety concerns for facial topography customized 3D-printed N95 filtering face-piece respirator produced for the COVID-19 pandemic: initial step is respiratory fit testing. Int J Oral Maxillofac Surg. 2020. Ahead of print. DOI: 10.1016/j.ijom.2020.08.017.

31. AATCC TM79-2010e2(2018)e, AATCC Website. Available at: https://members.aatcc.org/store/tm79/499/. Accessed on October 2, 2020.

32. Daerr A, Mogne A. Pendent_Drop: An ImageJ Plugin to Measure the Surface Tension from an Image of a Pendent Drop. *J Open Res Softw*. 2016; 4: e3.

Figure Legends

Figure 1. Overview of essential surgical N95 attributes.

Figure 2. The 5 designs are displayed with an image of them on a user in the second column, and the filter material used in the second column. The last two columns present the respirators stratified by standardized face size of the user. Radial bar plots display Overall Fit Factor from the OSHA 7-minute standardized fit test for each design as well as the 3M N95 for regular and small size standardized users. Green bars represent passing scores, 100 or greater, while red bars indicate failing scores. Areas noted by users to leak air were highlighted.

Figure 3. Fit scores across the 6 scored OSHA fit test sections are displayed for each respirator. An overall fit factor of 100 is required to pass testing, however a respirator need not pass all fit testing segments as the total fit score is a weighted average of all segments.

Figure 4. (a) Quality factor, (b) filtration efficiency (primary y-axis, red), and pressure drop (secondary y-axis, blue) observed for materials tested with an air flow face velocity of 7.6 ± 0.1 cm/s and 300 nm challenge NaCl particles. Error bars are 95% confidence intervals for mean values. 95% filtration efficiency is marked as a dashed red line.

Figure 5. Fabric characterization: Wettability and splatter testing. **A**. Wetting: Optical images of the two tested fabrics (Halyard and Filti), along with images of milk droplets with advancing contact angles of 120° and 127°, respective. Visible holes pin the liquid (receding contact angles: 0°) and are a possible weak point for liquid penetration. **B**. Repellency: Splatter testing, *i.e.*,

resistance to high-velocity liquid jet penetration (test liquid: whole milk at 4.5, 5.5, and 6.35 m/s), for single (left half-circle) and double (right half-circle) layers of Halyard and Filti fabrics. Red indicates repellency failure, *i.e.*, penetration of liquid through the fabric layer(s). Green indicates a passed test, if the majority of sampled fabrics did not show milk break-through. **C**. Multilayer: Optical image of the front (top) and inter-layer (bottom) surfaces after liquid jet impingement. Milk (dyed with red food color) penetrated the first layer and deposited on the underlying layer, but did not break through the second layer.

Supplemental Figure 1. Lines represent combinations of material filtration efficiency performance (%) and leakage (ie. around the face seal or through defects; % of flowrate) which result in a given fit factor.

Supplemental Figure 2. Face velocity of 85 L/min as a function of filtration surface area.

Supplemental Figure 3. For several materials, pressure drop is modeled as a function of face velocity. Vertical lines represent the characteristic face velocity for 85 L/min flowrate through the filtration area of the improvised designs.

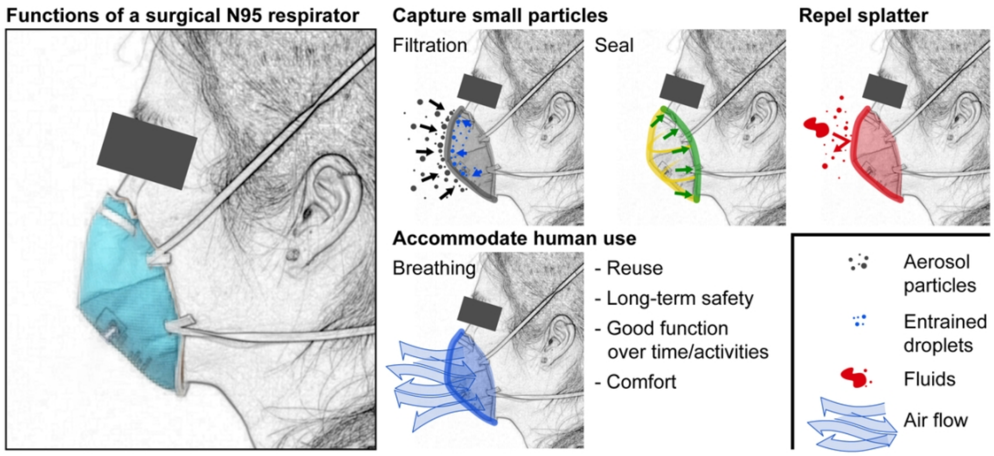

Figure 1. Overview of essential surgical N95 attributes.

107x49mm (300 x 300 DPI)

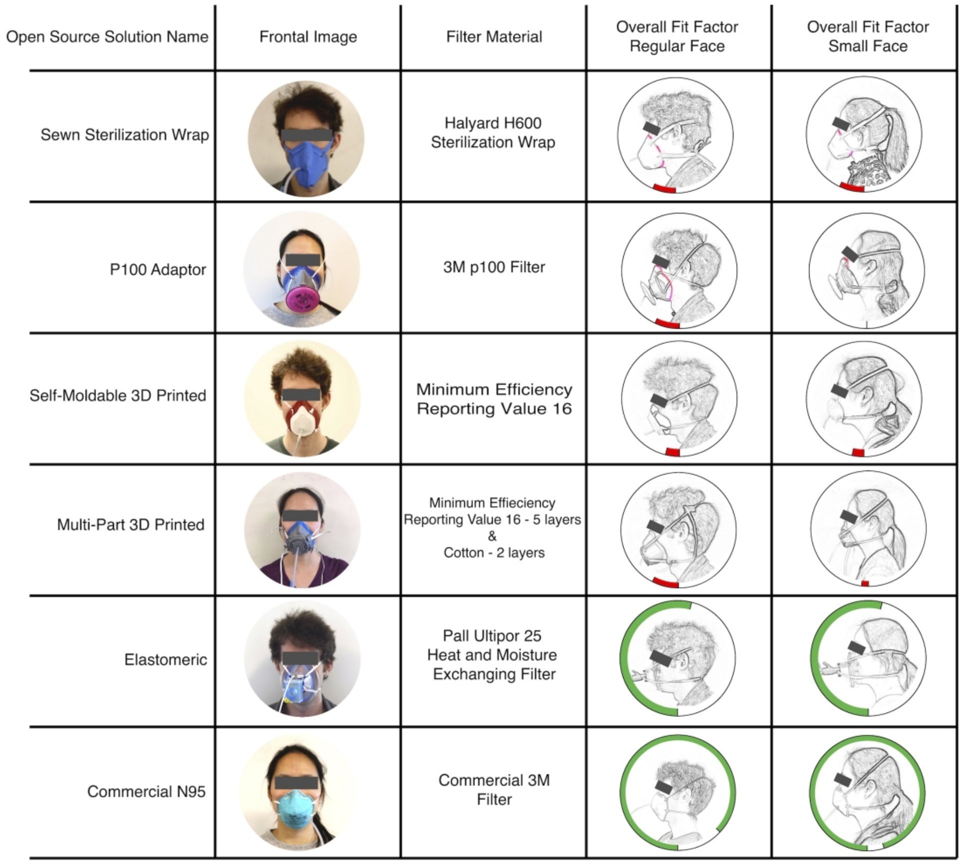

Figure 2. The 5 designs are displayed with an image of them on a user in the second column, and the filter material used in the second column. The last two columns present the respirators stratified by standardized face size of the user. Radial bar plots display Overall Fit Factor from the OSHA 7-minute standardized fit test for each design as well as the 3M N95 for regular and small size standardized users. Green bars represent passing scores, 100 or greater, while red bars indicate failing scores. Areas noted by users to leak air were highlighted.

254x221mm (300 x 300 DPI)

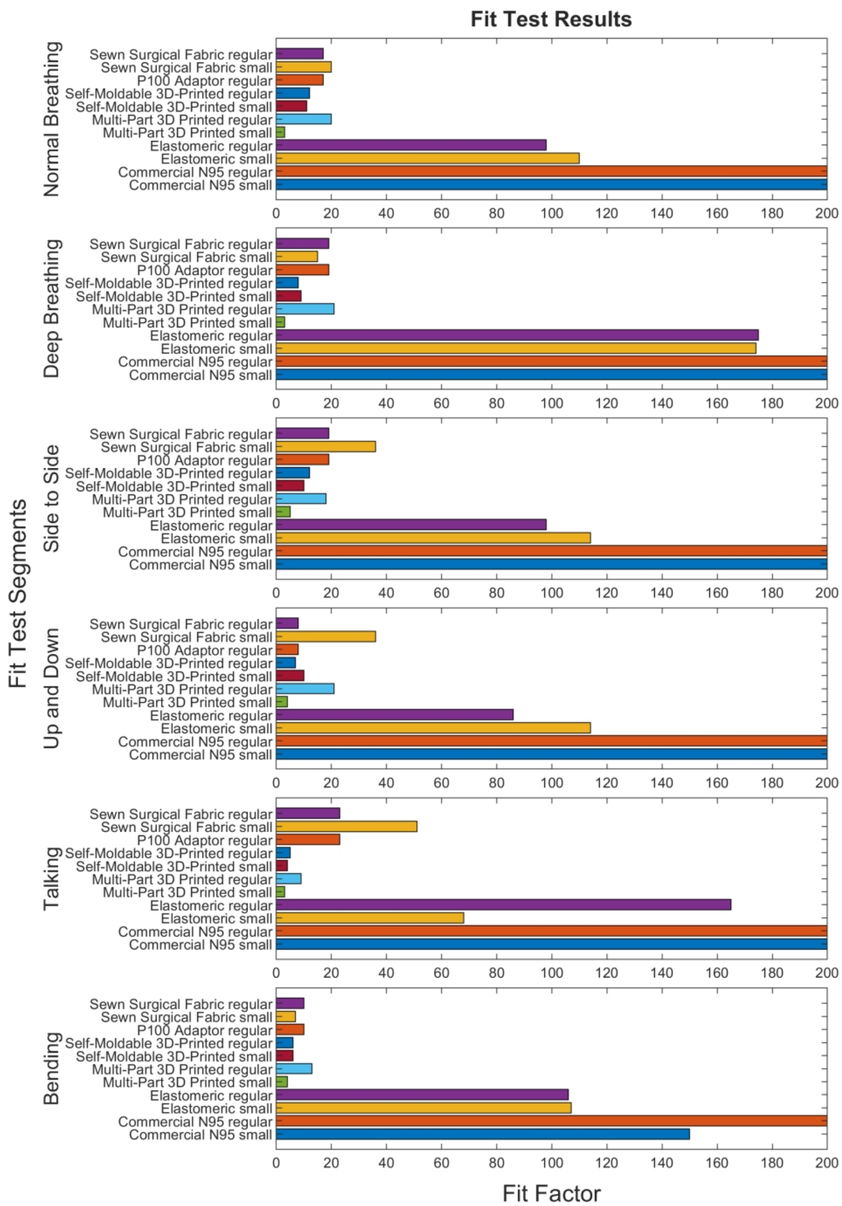

Figure 3. Fit scores across the 6 scored OSHA fit test sections are displayed for each respirator. An overall fit factor of 100 is required to pass testing, however a respirator need not pass all fit testing segments as the total fit score is a weighted average of all segments.

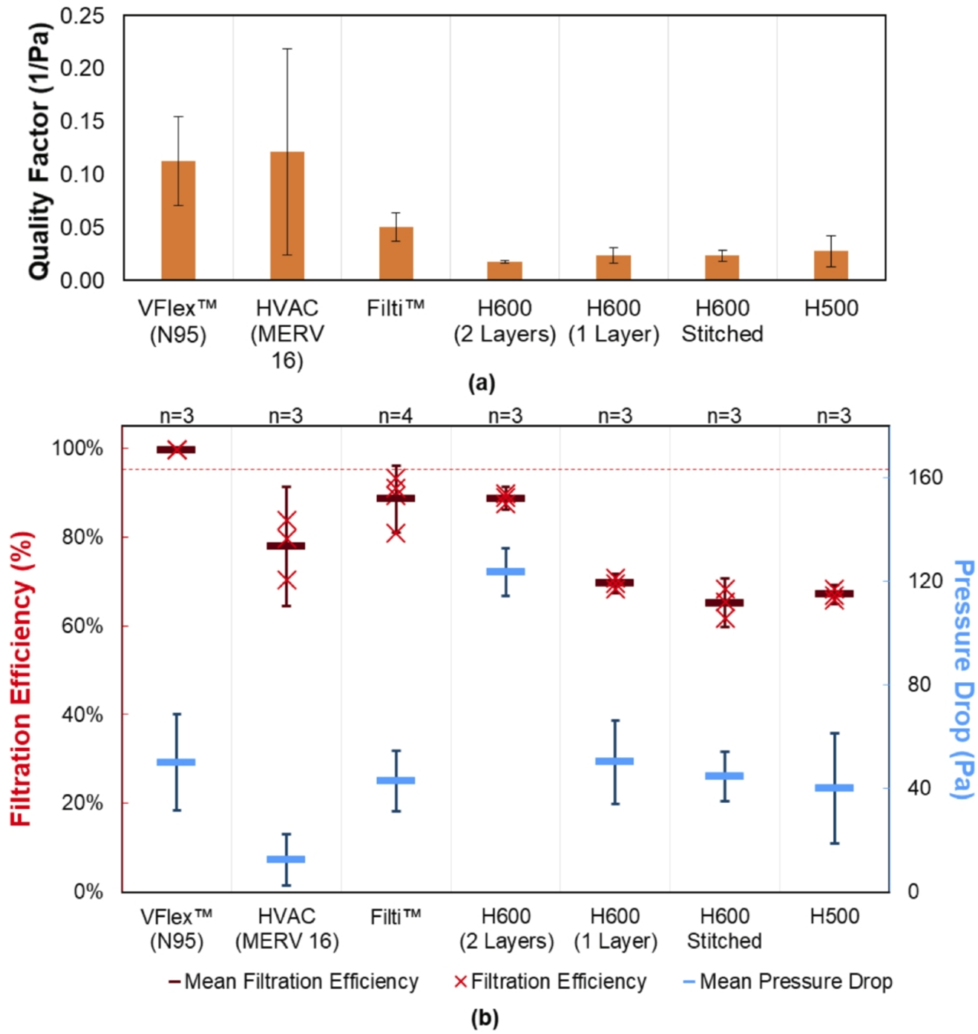

Figure 4. (a) Quality factor, (b) filtration efficiency (primary y-axis, red), and pressure drop (secondary y-axis, blue) observed for materials tested with an air flow face velocity of 7.6 ± 0.1 cm/s and 300 nm challenge NaCl particles. Error bars are 95% confidence intervals for mean values. 95% filtration efficiency is marked as a dashed red line.

205x220mm (300 x 300 DPI)

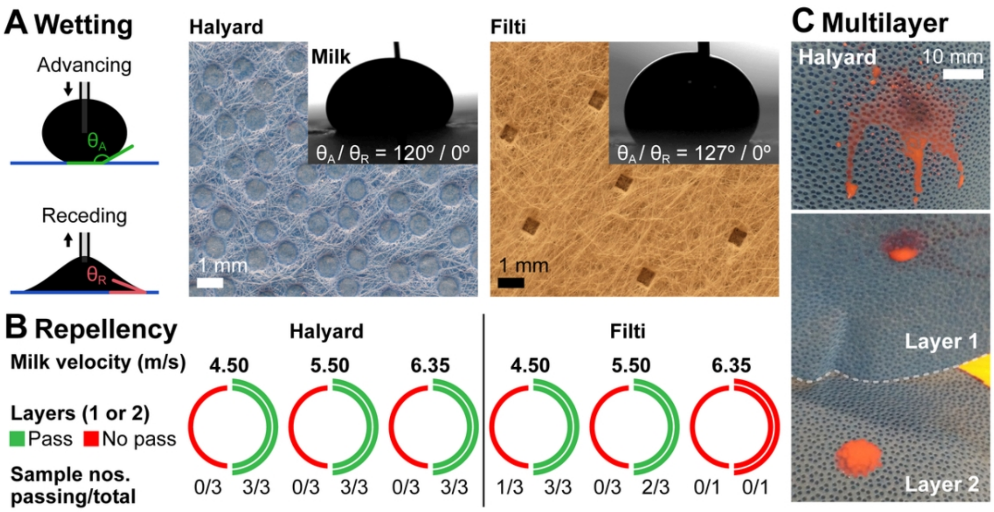

Figure 5. Fabric characterization: Wettability and splatter testing. A. Wetting: Optical images of the two tested fabrics (Halyard and Filti), along with images of milk droplets with advancing contact angles of 120° and 127°, respective. Visible holes pin the liquid (receding contact angles: 0°) and are a possible weak point for liquid penetration. B. Repellency: Splatter testing, i.e., resistance to high-velocity liquid jet penetration (test liquid: whole milk at 4.5, 5.5, and 6.35 m/s), for single (left half-circle) and double (right half-circle) layers of Halyard and Filti fabrics. Red indicates repellency failure, i.e., penetration of liquid through the fabric layer(s). Green indicates a passed test, if the majority of sampled fabrics did not show milk break-through. C. Multilayer: Optical image of the front (top) and inter-layer (bottom) surfaces after liquid jet impingement. Milk (dyed with red food color) penetrated the first layer and deposited on the underlying layer, but did not break through the second layer.

103x53mm (300 x 300 DPI)

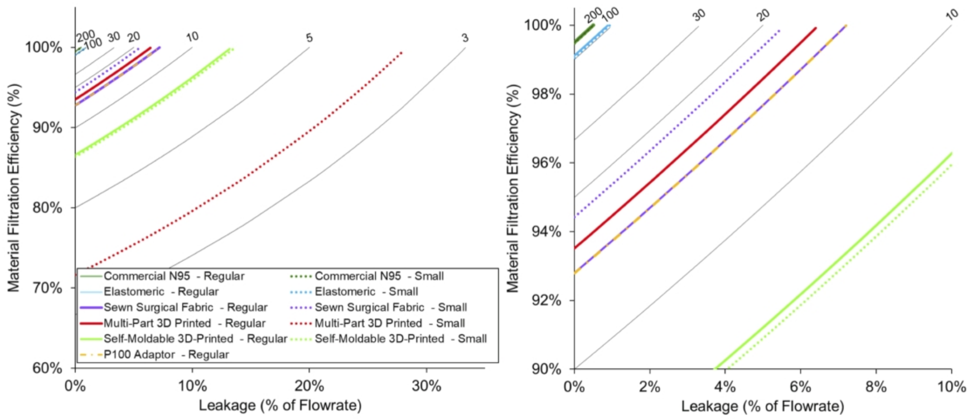

Supplemental Figure 1. Lines represent combinations of material filtration efficiency performance (%) and leakage (ie. around the face seal or through defects; % of flowrate) which result in a given fit factor.

270x116mm (300 x 300 DPI)

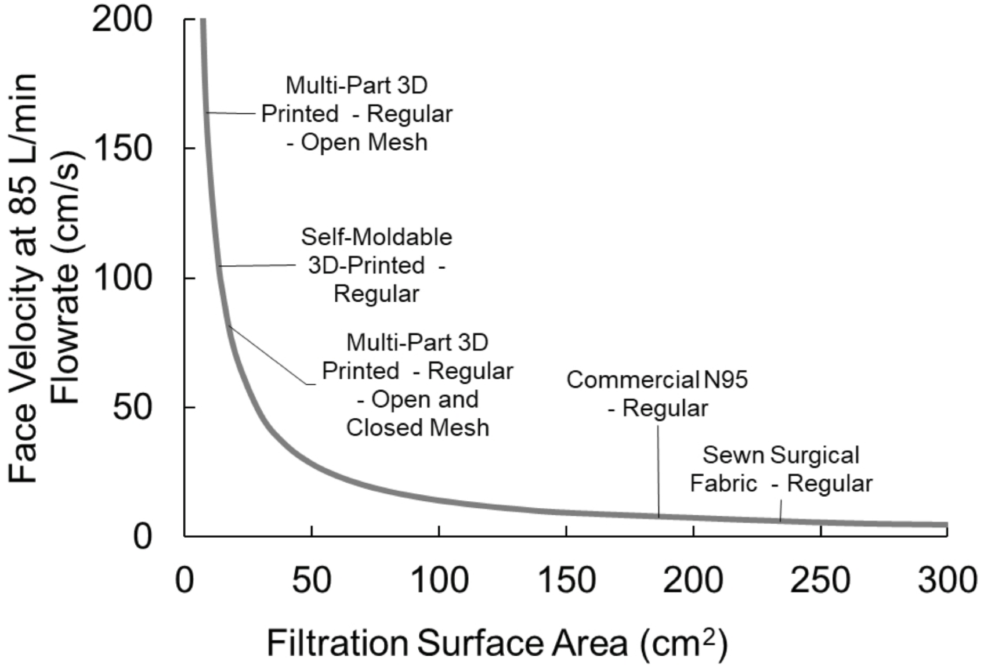

Supplemental Figure 2. Face velocity of 85 L/min as a function of filtration surface area.

264x186mm (300 x 300 DPI)

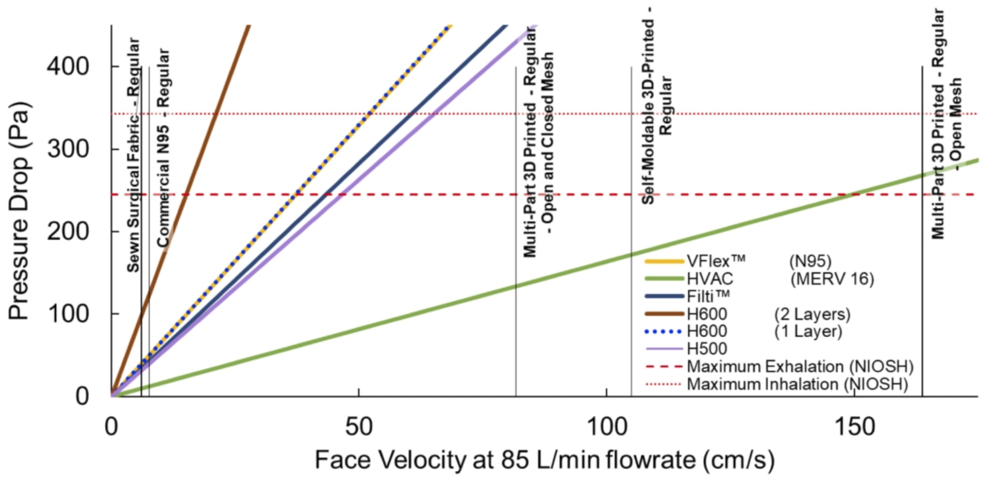

Supplemental Figure 3. For several materials, pressure drop is modeled as a function of face velocity. Vertical lines represent the characteristic face velocity for 85 L/min flowrate through the filtration area of the improvised designs.

267x132mm (300 x 300 DPI)

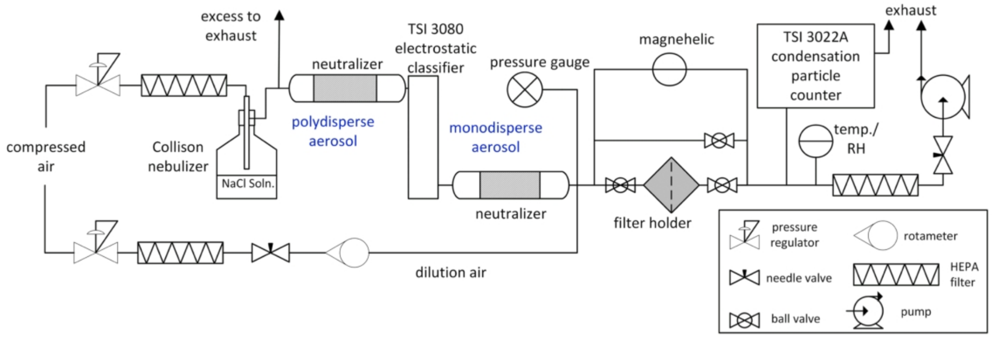

(Note to reviewers/editors - this figure is NOT referenced in the main document, only in the supplementary data document). Supplemental Figure 4. Flow diagram of the aerosol filtration testing station.

269x96mm (300 x 300 DPI)

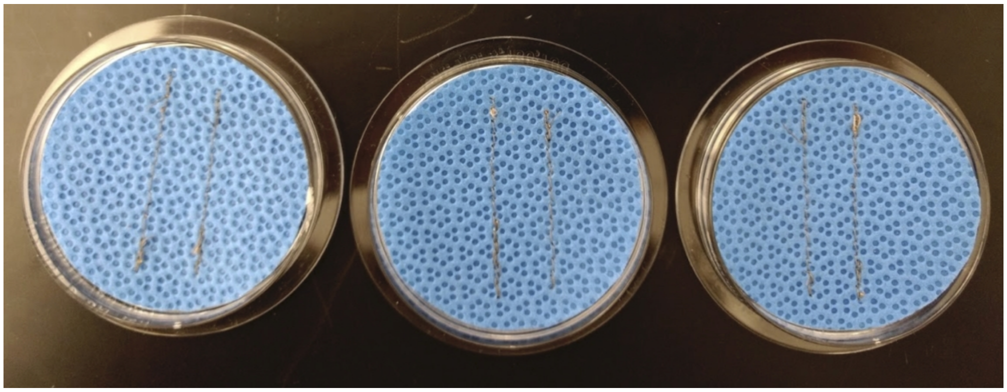

(Note to reviewers/editors - this figure is NOT referenced in the main document, only in the supplementary data document). Supplemental Figure 5. 47 mm discs were cut from H600 sterilization wrap fabric sheets (Halyard Health, Alpharetta, GA) and stitched with two straight lines using a sewing machine. The total length of stitching on each of the three filters was 6.7, 6.5, and 7.0 cm.

271x104mm (300 x 300 DPI)

Supplementary Mask Fabrication Methods

For 3D printed respirator designs, a number of different 3D printers and materials were used depending on availability. For sewn respirators, traditional sewing machines were used by experienced sewers. In all cases, fabrication followed the process defined in the online instructions. Detailed fabrication procedures for the five designs, named as follows in the main text: P100 Adaptor**,** Multi-part 3D Printed Mask, Sewn Sterilization Wrap, Commercial Elastomeric Respirator, Self-Moldable 3D Print. All links were retrieved on May 1, 2020.

Sewn Sterilization Wrap

The Florida mask pattern and instructions were downloaded from the University of Florida Department of Anesthesiology website.[1] Two layers of Halyard 600 sterilization wrap (Halyard, Alpharetta, GA) was cut according to the pattern downloaded and printed from the website. The masks were assembled with a Janome Memory Craft (Janome, Tokyo, Japan) home sewing machine according to the detailed instructions provided. Spandex elastic 3/8 inch (0.952 cm) wide was attached at the specified locations.

P100 Adaptor

Manufacture of the "P100 Adaptor" mask followed open source instructions created at the Barrow Innovation Center (Phoenix, AZ).[2] Mask parts were produced by fused deposition modeling 3D printing and silicone casting for fit. Parts were printed in PLA (grey stock 1.75 mm from Prusa) with 20% infill and a shell thickness of 4 perimeters using a .4 mm nozzle on a Prusa i3 MK3s. The print layer height was .2 mm thickness. Print temperature was 200°C with a print bed temperature of 70°C. A soldering iron was used to melt perforations in 3D printed mask perimeter. A mold was created from a production staff member's face, encasing the printed shell of the mask with clay. This clay mold was then removed, and a silicone seal was cast. Assembly of the mask required manually clearing the holes in the plastic shell and trimming clearance for elastic head straps to pass silicone seal. An O-ring seal was applied prior to attachment of a p100 filter.

Specifications were followed as described in the document from the Barrow Innovation Center, with a few exceptions as follows. The silicone mold as described was observed to be too thick to obtain a completed seal, so the edge of mold was sculpted back for a better fit. Moreover, the seal as described did not stay adhered to the mask shell on first casting and had to be glued after removal from mold. Although the end user would ideally be present for mask production to ensure personalized fit, this was not possible in our fabrication process, and masks were molded to the face of a production staff member.

Self-Moldable 3D Print

"Self-Moldable 3D Print" masks designs were obtained from open source instructions provided by Make the Masks.[3] 3D printer files were formatted in Simplify3D (Simplify3D, Cincinnati, OH) for use on the Fusion3 F410 (Fusion 3D, Greensboro, NC) single filament printer with a 0.4 mm diameter print head and standard 1.75 mm PLA. Head temperature was set at 240°C. Test prints priors were conducted at infills of 10%, 15%, 20% and 25% with aspect ratios of 90%, 95%, and 100%, corresponding to small, medium, and large face sizes. These test prints were sanded, cleaned, and test fit to gauge pliability under heat molding as outlined by the designers. Lower infills yielded more pliable masks but ran the risk of allowing perforations in the print layers that compromised the integrity of the mask. After these preliminary test prints, prototype samples were printed with a print head temperature of 230°C, with extrusion and print speeds lowered to 90%, and monitored for the duration of the print to ensure quality of layer adhesion at an infill of 15% in aspect ratios of 90% and 100%. Masks were individually molded to user faces using a hot water dip and adequate molding was established by forcibly exhaling against a blocked filter to identify points of air leak prior to quantitative testing.

Multi-part 3D Printed Mask

Manufacture of the "Multi-part 3D Printed Mask" closely followed open source instruction provided online by River City Labs.[4] Parts were printed in PLA (grey stock 1.75 mm from Prusa, Prague, Czech Republic) with 20% infill and a shell thickness of 3 perimeters using a .4 mm nozzle on a Prusa i3 MK3s. The print layer height was .2 mm thickness. Print temperature was 200°C with a print bed temperature of 70°C. Notably, a deviation in the printing process from the instructions was use of PLA rather than Polyethylene Terephthalate Glycol-modified (PETG) due to supply availability. For filtration material, Merv 13 (AAF International, Doraville, GA) was substituted for Merv 16 due to local supply limitations. After 3-D printing from the file provided and testing the seal mold, adjustments to the external geometry were needed to enable fitting. To address this, an alternative seal mold external geometry was developed to allow for better closure, but this still failed to yield a perfect seal. Seals did not self-retain on the contoured mask shell due to low elasticity of the seals, requiring gluing to the shell edge. Additionally, extensive hand finishing was not performed on exterior parts or on threads of articulating parts due to increasing thread tolerance and worsening seal.

Commercial Elastomeric Respirator

Instruction for fabrication were obtained from open source documents provided on the Boston Children's Hospital Website.[5] The "Commercial Elastomeric Respirator" was fabricated by mounting a Ultipor 25 Ventilator Inline Bacterial/Viral Filter (Pall Corporation, Westborough, MA) on an anesthesia face mask with one end open to the environment. A face piece-filter adapter with integrated sampling port was 3D printed of polylactic acid (PLA) using fused deposition modeling (Prusament PLA; Prusa i3 MK3S, Prusa Research, Prague, CZ). The sampling port was tapped to receive a 1/4 inch-28 compression fitting to seal around fluorinated ethylene propylene (FEP) tubing with an outer diameter of 1/8 in (3.12 mm). The mask was then secured using elastic straps attached to the 4-pronged ring surrounding the inflow and outflow tract.

Supplementary Splatter testing Methods

For splatter testing, a Nordson EFD ValveMate 8000 (Nordson Corporation, Westlake, OH) with a 741V pneumatic valve generated the liquid jet. Fabrics, either as a single or a double layer, were secured using a 1/16 inch (0.159 cm) rubber cuff over a polyethylene terephthalate (PET) 3D printed backing form with the standard-specified dimensions. A 0.25 inch (0.635 cm) centering hole, drilled into an acrylic sheet, was placed approximately 0.5 inches (1.27 cm) from the respirator surface, and the valve with an 18 gauge needle was placed at a distance of 12 inches (30.5 cm). After impingement, fabrics were visually inspected for liquid penetration.

Supplementary Filtration Methods

A flow diagram of the particle testing station is provided in Figure S1. Sample discs of 47 mm were extracted directly from the mask or the sourced material sheet and placed in a stainless steel in-line filter holder (Pall #2220, Pall Corporation, Westborough, MA), which exposed a circular area of 35 mm diameter during filtration testing. A polydisperse NaCl aerosol was produced from a 1.0 %wt. NaCl solution in DI water using a Collison Nebulizer (CH Technologies) and an in-line custom diffusion dryer, with a pressure of 8 psig (55.2 kPa) and a flow rate of 6 liters per minute (LPM). The aerosol was then passed through an electrostatic classifier (TSI Inc., Model 3080, Shoreview, MN, with long differential mobility analyzer (DMA) column, operated with a sheath flowrate of 5 LPM and an aerosol flow rate of 1.46 LPM ± 0.04, which was set by controlling the pressure at the exit of the DMA by continually adjusting the needle valve to vacuum) to select particles based on mobility in the electric field with a peak mobility size of 300 nm mean diameter. Electric mobility is proportional to the ratio of particle charge and aerodynamic diameter (equivalent to diameter for spherical particles), such that for a given diameter setpoint, a set of particles of increasing diameter and discrete charge (ie. +1, +2, etc.) will be selected by the DMA. Since the mode of the nebulizer size distribution is less than the 300 nm setpoint and since the aerosol is neutralized prior to the DMA, the singly charged particles (with 300 nm diameter mode) will predominate. After the classifier, the aerosol was neutralized a second time by flowing through a tube with two imbedded Po-210 strips (NRD Staticmaster 2U500, Grand Island, NY) and then diluted with HEPA-filtered house air. In the case of samples at 4.38±0.05 LPM (corresponding to 7.6±0.1 cm/s face velocity to the exposed filter area), an additional 2.92 LPM of using HEPA-filtered house air was added to achieve a final particle number concentration in the range of 3000 - 4000 particles per cubic centimeter. To determine the filtration efficiency, the concentrations of particles upstream and downstream of the filter were measured using a continuous condensation particle counter (TSI Inc., Model 3022A). Upstream and downstream particle concentrations were measured in immediate succession to mitigate impact of drift in nebulizer output over time. The flow through the filter material was varied to achieve a range of face velocities. The pressure drop across the filter material was measured with a magnehelic differential pressure gauge (Dwyer, Michigan City, IN) and the temperature and relative humidity of the gas passed through the filter was measured with an industrial probe (Dwyer HHT Series). Relative humidity and temperature were not actively controlled and were within the range of 8 and 21 % relative humidity and 19.4 and 21.1°C for the results presented here.

<u>*Methods of calculation*</u>

Particle filtration efficiency for a single punch was calculated from the unfiltered and filtered particle concentrations ($C_{Unfiltered}$ and $C_{Filtered}$ respectively):

$$(Filtration\ Efficiency) = 1 - \frac{C_{Filtered}}{C_{Unfiltered}}.$$

$C_{Unfiltered}$ and $C_{Filtered}$ were calculated as the mean of replicate measurements through the bypass line and filter respectively for the same punch:

$$C = \frac{1}{J}\sum_{j=1}^{J}\bar{x}_j$$

where $\bar{x}_j$ is the j^{th} replicate measurement (of a total of J) for a given condition (filtered or unfiltered) and is calculated from the mean concentration (#/cc) recorded by the condensation particle counter (CPC) (for at least 30 s at 1 s time resolution):

$$\bar{x}_j = \frac{1}{n_{CPC}} \sum_{i=1}^{n_{CPC}} x_i$$

where x_i is the i^{th} raw concentration datum (of a total of n_{CPC} data) recorded by the CPC. $C_{Unfiltered}$ was also corrected for particle penentration (99.4% ± 2.4) through the empty filter holder relative to the bypass line:

$$C_{Unfiltered} = (99.4\%) \cdot \frac{1}{J} \sum_{j=1}^{J} \bar{x}_j$$

The uncertainty in filtration efficiency is the combined uncertainty of the two measurements as well as the uncertainty in the measurement of particle penetration through the empty filter holder:

$$S_{Efficiency} = (1 - Filtration\ Efficiency) \sqrt{\left(\frac{2.4\%}{99.4\%}\right)^2 + \left(\frac{S_{Unfiltered}}{C_{Unfiltered}}\right)^2 + \left(\frac{S_{Filtered}}{C_{Filtered}}\right)^2}.$$

The uncertainty of the unfiltered or filtered particle concentration ($S_{unfiltered}$, $S_{filtered}$) for a punch was calculated as the combined error from the maximum relative CPC variability (S_{CPC}) observed for that condition and punch and the variability between replicate measurements of the filtered or unfiltered particle concentrations (S_{Punch}):

$$S = \sqrt{S_{CPC}^2 + S_{Punch}^2}$$

$$S_{CPC} = max\left(\frac{s_{CPC,j}}{\bar{x}_j \sqrt{n_{CPC}}}\right) \times C$$

where n_{CPC} is the number of CPC measurements and $s_{CPC,j}$ is the standard deviation of the raw CPC data:

$$s_{CPC,j} = \sqrt{\frac{\sum_{i=1}^{n_{CPC}} (x_i - \bar{x}_j)^2}{n_{CPC} - 1}}$$

Given the evolving and urgent demand for this data, the number of replicates of measurements of $C_{Unfiltered}$ and $C_{Filtered}$ for a single punch ($n_{condition,\,unfiltered}$ and $n_{condition,\,filtered}$) varied from one unfiltered and one filtered measurement to three unfiltered and two filtered measurements (with the mean of each condition used to calculate filtration efficiency). These replicate measurements were always performed in immediate succession to mitigate any long-term nebulizer output drift. In cases where the unfiltered or filtered particle concentration $\bar{x}_j$ was measured multiple times for a single punch (with the mean value C used to calculate the particle capture efficiency), S_{Punch} was calculated as the standard error of the mean of these replicate measurements:

$$S_{Punch} = \frac{\sqrt{\frac{\sum (y_j - \bar{y})^2}{n_{condition} - 1}}}{\sqrt{n_{condition}}}$$

where $n_{condition}$ is the number of replicate measurements for that condition and punch.

As discussed previously, for several punches, only a single unfiltered or filtered measurement were taken. Since a standard error cannot be computed for a single replicate, we estimated S_{Punch} using the standard error of an estimate calculated for the regression of repeat measurements (n=16 for unfiltered measurements, n=13 for filtered measurements) versus time in a separate test with the same sample flowrate and diameter setpoint. This approach yields estimates of $\frac{S_{Punch,filtered}}{C}$ of 1.43% and $\frac{S_{Punch,unfiltered}}{C}$ of 0.93%.

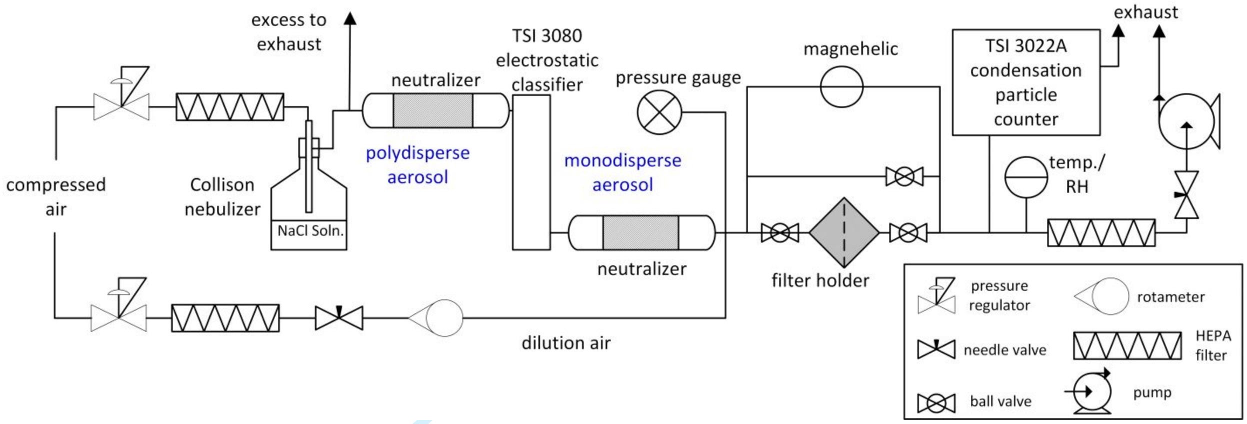

Supplemental Figure 4. Flow diagram of the aerosol filtration testing station.

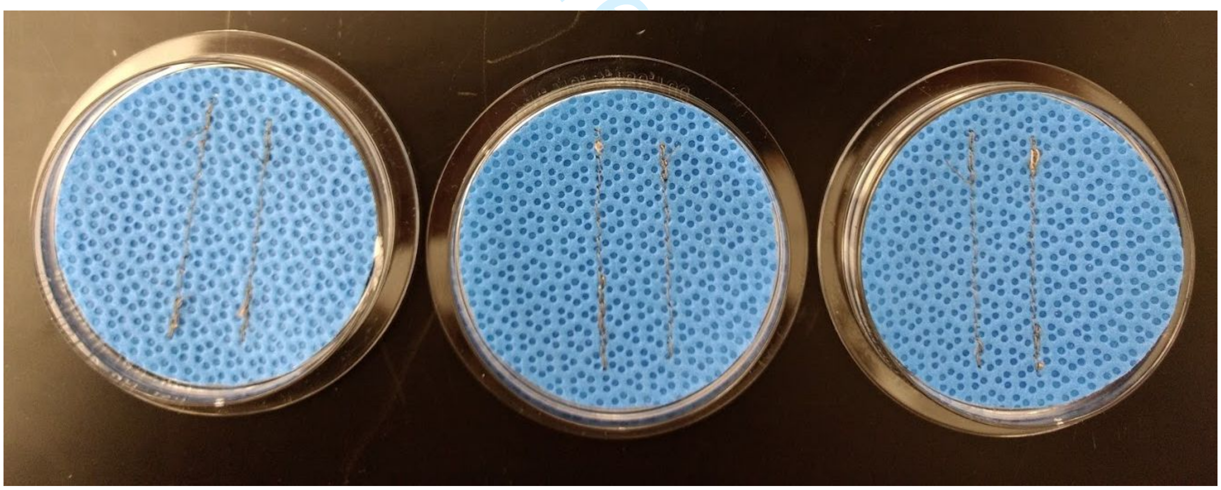

Supplemental Figure 5. 47 mm discs were cut from H600 sterilization wrap fabric sheets (Halyard Health, Alpharetta, GA) and stitched with two straight lines using a sewing machine. The total length of stitching on each of the three filters was 6.7, 6.5, and 7.0 cm.

Supplementary Discussion of Individual Discussion of Respirators

Sewn Sterilization Wrap

The sewn sterilization wrap was well tolerated by participants who noted its breathability and easily understandable speech. Nevertheless, the respirator presented a poor seal with multiple points of air leak including the nose, chin and cheeks. The respirator surface area is small compared to many currently marketed duckbill respirators and these leaks may be improved by extending the material outward across the cheeks and further below the jawline. Additionally, users noted difficulty with tightening the respirator straps due to lack of elasticity, with additionally restricted head motion when the lower strap was tightened with the head in a neutral position and the participants were instructed to look upward. Circumferential seal can be potentially improved with more elastic straps to provide additional tension to the sides of the respirator.

P100 Adaptor

Due to fabrication limitations users were not present for silicone molding and fitting and consequently the respirator was unable to be tested on a small sized user due to gross mismatch in size and circumferential lack of seal. Users noted easy breathability, but the hard-plastic design contacting the chin created discomfort while talking and acted as a lever during upward head motion reducing perceived seal. The strength of the straps was also insufficient to support the weight of the respirator with the attached filter and caused pulling away from the face during downward movements. While ideally respirators would have been molded individually to the end users this highlights a crucial challenge in widespread implementation.

Self-Moldable 3D Print

The Self-Moldable 3D Print respirator was well tolerated with easy breathability and speech comprehension. Users performed fit testing prior to individualized heat molding (described in supplementary methods) and noted that perceived air leaks were resolved with molding, however fit factor was not improved. Without fit testing this may lead to a false assurance of respirator fit and underscores the importance of proper fit testing. Additionally, users found the heat molding process to be difficult and cumbersome and a potential challenge to widespread implementation.

Multi-part 3D-Printed Mask

The multi-part 3D-printed respirator was poorly tolerated by users due to discomfort at the nose bridge and cheek bones from the hard-plastic fit as well as highly muffled and near incomprehensible speech. The multi-part design introduced several potential locations for air leak, most notably the lack of an O-ring rubber seal between the threads of the 3D respirator shell and filter housing. On forceful exhalation users noted potential air leak around the filter. Material and fabrication constraints are discussed in the supplemental methods and represent challenges with wide implementation of the respirator solution.

Commercial Elastomeric Respirator

The Commercial Elastomeric Respirator was poorly tolerated by users, both commented on discomfort at the bridge of the nose which may be attributable to greater tension on the upper strap necessary to achieve good fit. This was partially relieved by increasing inflation of the respirator, however fully inflating the respirator for user comfort compromised fit during real-time testing. Additionally, users noted difficulty with talking due to tension placed on the jaw. Speech was highly muffled and difficult to understand. Furthermore, the weight of the filter caused subjective difficulty with fit during head motion and may explain the inconsistency in fit across fit test segments. Additionally, users commented on the difficulty of adjusting respirator tightness due to the high elasticity of the straps, which was necessary to counteract the high weight of the respirator. Iterations of this respirator with a single filter were found to be significantly more difficult to breathe through compared to those with a bifurcated adaptor that allowed for attachment of two separate filters.

REFERENCES

7. Mask Alternative. University of Florida College of Medicine Department of Anesthesiology Website. Available at: https://anest.ufl.edu/clinical-divisions/mask-alternative/#prototype2 Accessed on October 2, 2020

8. 3D Printed N95 Replacement Mask. Barrow Neurological Institute Website. Available at: https://www.barrowneuro.org/get-to-know-barrow/barrow-innovation-center-2/3d-printed-n95-mask/ Accessed October 2, 2020.

9. The Montana Mask. Make The Masks Website. Available at: https://www.makethemasks.com/ Accessed October 2, 2020.

10. The "MalaMask" Project (N95 Alternative Filter). River City Labs Website. Available at: https://wiki.rivercitylabs.space/covid-19/3d-printed-masks Accessed on October 2, 2020.

11. Surgical Innovation Fellowship. Boston Children's Hospital Website. Available at: http://www.childrenshospital.org/research/departments-divisions-programs/departments/surgery/surgical-innovation-fellowship Accessed on October 2, 2020

BMJ Open

Protection levels of N95-level respirator substitutes proposed during the COVID-19 pandemic: safety concerns and quantitative evaluation procedures

Journal:	*BMJ Open*
Manuscript ID	bmjopen-2020-045557.R1
Article Type:	Original research
Date Submitted by the Author:	30-Jun-2021

Complete List of Authors:	Ballard, David; Washington University in St Louis School of Medicine Mallinckrodt Institute of Radiology, Dang, Audrey ; Washington University in St Louis, Department of Energy, Environmental and Chemical Engineering Kumfer, Benjamin ; Washington University in St Louis, Department of Energy, Environmental and Chemical Engineering Weisensee, Patricia; Washington University in St Louis, Department of Mechanical Engineering & Materials Science Meacham, J; Washington University in St Louis, Department of Mechanical Engineering & Materials Science Scott, Alex; Washington University in St Louis, School of Medicine Ruppert-Stroescu, Mary; Washington University in St Louis, Sam Fox School of Design and Visual Arts Burke, Broc; Washington University in St Louis, Department of Anesthesiology Morris, Jason; Washington University in St Louis, School of Medicine Gan, Connie; Washington University in St Louis, School of Medicine Hu, Jesse; Washington University in St Louis, School of Medicine King, Bradley; Washington University in St Louis, Department of Environmental Health & Safety Jammalamadaka, Udayabhanu; Washington University in St Louis, Mallinckrodt Institute of Radiology Sayood, Sena; Washington University in St Louis, Division of Infectious Diseases Liang, Stephen; Washington University in St Louis, Division of Infectious Diseases Choudhary, Shruti; Washington University in St Louis, Department of Energy, Environmental and Chemical Dhanraj, David ; Washington University in St Louis, Department of Energy, Environmental and Chemical Maranhao, Bruno; Washington University in St Louis, Department of Anesthesiology Millar, Christine; Memorial Hospital Belleville, Department of Anesthesiology Bertroche, J; Washington University in St Louis, Department of Otolaryngology-Head & Neck Surgery Shomer, Nirah; Washington University in St Louis, Division of Comparative Medicine Woodard, Pamela; Washington University in St Louis School of Medicine

	Mallinckrodt Institute of Radiology Biswas, Pratim; Washington University in St Louis, Department of Energy, Environmental and Chemical Engineering Axelbaum, Richard; Washington University in St Louis, Department of Energy, Environmental and Chemical Engineering Genin, Guy; Washington University in St Louis, Department of Mechanical Engineering & Materials Science Williams, Brent; Washington University in St Louis, Department of Energy, Environmental and Chemical Meacham, Kathleen; Washington University in St Louis, Department of Anesthesiology
Primary Subject Heading:	Occupational and environmental medicine
Secondary Subject Heading:	Public health, Anaesthesia, Infectious diseases
Keywords:	COVID-19, OCCUPATIONAL & INDUSTRIAL MEDICINE, Health & safety < HEALTH SERVICES ADMINISTRATION & MANAGEMENT, PREVENTIVE MEDICINE, Adult anaesthesia < ANAESTHETICS

Protection levels of N95-level respirator substitutes proposed during the COVID-19 pandemic: safety concerns and quantitative evaluation procedures

David H. Ballard, MD[1]; Audrey J. Dang BE[2]; Benjamin M. Kumfer, DSc[2]; Patricia B. Weisensee, PhD[3]; J. Mark Meacham PhD[3]; Alexander R Scott, BA, BS[4]; Mary Ruppert-Stroescu, PhD[5] Broc A. Burke, MD, PhD[6]; Jason A. Morris, BS[4]; Connie Gan, BS[4]; Jesse Hu, BS[4]; Bradley King[7]; Udayabhanu Jammalamadaka, PhD[1]; Sena Sayood, MD[8]; Stephen Y. Liang, MD[8]; Shruti Choudhary, BS[2]; David I A, Dhanraj, BS[2]; Bruno Maranhao, MD, PhD[6]; Christine Millar, MD[9]; J. Tyler Bertroche, MD[10]; Nirah H Shomer, DVM, PhD, DACLAM[11]; Pamela K Woodard, MD[1]; Pratim Biswas, PhD[2]; Richard L. Axelbaum, PhD[2]; Guy M. Genin, PhD[3,12,13]; Brent J. Williams, PhD[2]; Kathleen W. Meacham, MD, PhD[6]

1- *Mallinckrodt Institute of Radiology, Washington University School of Medicine, St. Louis, MO*
2- *Department of Energy, Environmental and Chemical Engineering, Washington University in St Louis, St. Louis, MO*
3- *Department of Mechanical Engineering & Materials Science, Washington University in St. Louis, MO*
4- *School of Medicine, Washington University School of Medicine, St. Louis, MO*
5- *Sam Fox School of Design and Visual Arts, Washington University in St. Louis, St Louis, MO*
6- *Department of Anesthesiology, Washington University School of Medicine, St Louis, MO*
7- *Department of Environmental Health & Safety, Washington University School of Medicine, St. Louis, MO*
8- *Division of Infectious Diseases, Washington University School of Medicine, St. Louis, MO*
9- *Department of Anesthesiology, Memorial Hospital Belleville; Belleville, IL*
10- *Department of Otolaryngology-Head & Neck Surgery, Washington University School of Medicine, St Louis, MO*
11- *Division of Comparative Medicine, Washington University School of Medicine, St. Louis, MO*
12- *NSF Science and Technology Center for Engineering Mechanobiology, Washington University in St. Louis, St Louis, MO*
13- *Bioinspired Engineering and Biomechanics Center, School of Life Sciences and Technology, Xi'an Jiaotong University, China*

Correspondence to:

Brent Williams, PhD
Raymond R. Tucker Distinguished InCEES Career Development Associate Professor
Director, Atmospheric Chemistry and Technology Lab
Dept. of Energy, Environmental & Chemical Engr.
Washington University
St. Louis, Missouri, 63110
Email: brentw@wustl.edu
Phone: (314) 935-9279

Kathleen W. Meacham, MD PhD
Assistant Professor
Department of Anesthesiology
Washington University School of Medicine
660 South Euclid Ave, Campus Box 8054
St. Louis, Missouri, 63110
Email: meachamk@wustl.edu
Phone: (314) 393-4117; Fax: (314) 362-8334

Twitter handles: DHB (@DavidBallardMD), PKW (@PamelaWoodardp), PB (lab) (@AAQRL_Biswas)

Short title: Safety of public potential N95 respirator substitutes

Funding: This work was supported in part by a National Science Foundation Graduate Research Fellowship (DGE-1745038) and International Anesthesiology Research Society Mentored Research Award. BAB and KWM receive salary support from International Anesthesiology Research Society Mentored Research Award. AJD was supported by a National Science Foundation Graduate Research Fellowship (DGE-1745038). Any opinions, findings, and conclusions or recommendations expressed in this material are those of the authors and do not necessarily reflect the views of the National Science Foundation.

Competing Interests: All authors - No relevant disclosures related to the present study

Acknowledgements: The Washington University N95 design task force for their support and facilitating testing.

Manuscript Type: Original/Laboratory Investigation; Abstract Word Count: 295; Manuscript Word Count: 4,305; Numbers of Figures: 5; Supplemental Figure: 5; Supplemental Documents: 1 Supplemental Document with 2 Supplemental Figures and 1 Table

Keywords: COVID-19; N95 respirator; personal protective equipment; filtering facepiece respirator; 3D printing

Protection levels of N95-level respirator substitutes proposed during the COVID-19 pandemic: safety concerns and quantitative evaluation procedures

ABSTRACT

Objective: The COVID-19 pandemic has precipitated widespread shortages of filtering face-piece respirators (FFRs) and the creation and sharing of proposed substitutes (novel designs, repurposed materials) with limited testing against regulatory standards. We aimed to categorically test the efficacy and fit of potential N95 respirator substitutes using protocols that can be replicated in university laboratories.

Setting: Academic medical center with occupational health-supervised fit testing along with laboratory studies.

Participants: Seven adult volunteers with who passed quantitative fit testing for small (n=2) and regular (n=5) size commercial N95 respirators.

Methods: Five open-source potential N95 respirator substitutes were evaluated and compared to commercial National Institute for Occupational Safety and Health (NIOSH)-approved N95 respirators as controls. Fit testing using the 7-minute standardized Occupational Safety and Health Administration (OSHA) fit test was performed. In addition, protocols that can be performed in university laboratories for materials testing (filtration efficiency, air resistance, and fluid resistance) were developed to evaluate alternate filtration materials.

Results: Among five open-source, improvised substitutes evaluated in this study, only one (which included a commercial elastomeric mask and commercial HEPA filter) passed a standard

quantitative fit test. The four alternative materials evaluated for filtration efficiency (67% to 89%) failed to meet the 95% threshold at a face velocity (7.6 cm/s) equivalent to that of a NIOSH particle filtration test for the control N95 FFR. In addition, for all but one material, the small surface area of two 3D-printed substitutes resulted in air resistance that was above the maximum in the NIOSH standard.

Conclusions: Testing protocols such as those described here are essential to evaluate proposed improvised respiratory protection substitutes, and our testing platform could be replicated by teams with similar cross-disciplinary research capacity. Healthcare professionals should be cautious of claims associated with improvised respirators when suggested as FFR substitutes.

STRENGTHS AND LIMITATIONS

-Manufacturing of open source potential N95 respirator substitutes, quantitative fit testing, filtration testing, and material testing reflecting a method for others in a university lab setting to test N95 proposed substitute for a pandemic-related response

-Quantitative fit testing according to Occupational Safety and Health Administration provides an objective measure of how the N95 alternative substitute perform on individuals that passed fit testing on commercial N95 respirators

-Filtration data gives performance of improvised filter materials and how they perform at velocities relevant to normal breathing and filtering in the range of SARS-CoV-2 viral particles

-Limitation of the production of these open source substitutes were produced to the best of the author's understanding of posted instructions and did not attempt proposed substitutes to improve the mask designs

INTRODUCTION

Personal protective equipment (PPE) is critical for limiting infectious disease risk to clinicians. During the Coronavirus Disease 2019 (COVID-19) pandemic, the World Health Organization noted in February 2020 that the global stockpile of PPE was insufficient, particularly for masks and filtering facepiece respirators (FFRs).[1] In a survey in March 2020 by the Association for Professionals in Infection Control and Epidemiology, nearly half of respondents reported that their healthcare facility's N95 FFR supply was nearly or completely depleted.[2] To address these shortages, many institutions developed alternatives to commercial filtering facepiece (FFR) respirators to provide immediate stopgap solutions.[2-11] Some of these proposed substitutes were publicly disseminated, often with limited testing of key attributes including filtration, breathability, fit, and liquid fluid repellency.

Key functional attributes of N95 FFRs

In the United States, surgical N95 FFRs used by healthcare personnel are regulated by both the National Institute for Occupational Safety and Health (NIOSH) and the Food and Drug Administration (FDA). The surgical N95 respirator serves to protect wearers by filtering fine particles, providing a tight seal around the face, and repelling fluid splatter, while ensuring ease of breathing (**Figure 1**).[12, 13] Particle filtration efficiency is dependent on the size of the particle, the material properties of the respirator, and the face velocity at which the particle approaches the material; the face velocity depends on the user's instantaneous respiratory rate and the shape and size of the respirator itself. Respirator form must ensure that all breathed air passes through the filtration medium and does not leak from an edge. Lower flow resistance (larger surface area, material with lower pressure drop) reduces the work of breathing, mitigating wearer fatigue. The respirator must be comfortable, and respirator materials cannot pose health risks to the wearer (i.e., should not shed hazardous particles or fibers that can be inhaled). During crises, the respirator may need to function over periods of extended use and be reused; therefore, the respirator should be suitable for sterilization and maintain structural integrity. More specifically, supply of commercial N95 respirators has been conserved during the COVID-19 pandemic by multiple sterilization methods including hydrogen peroxide vapor, chlorine dioxide vapor, steam, ultra-violet radiation, heat, and isolation over time.[14-16] Finally, in the patient care environment, the filter material and/or an outer covering should repel high-velocity fluid splatter.

Due to the critical shortage of N95 respirators during the early COVID-19 pandemic, many institutions resorted to using locally improvised masks which have not undergone appropriate safety testing. As such, a discrepancy may exist between the respiratory protection actually provided by an improvised design and that the level of protection which healthcare workers would expect of a commercial respirator. Testing recently developed, open source designs intended as proposed substitutes for N95 respirators, we present our framework of establishing an institutional platform for evaluating these improvised designs and materials, including fit, filtration, and fluid repellancy testing. This framework could be replicated by collaborative teams with similar cross-disciplinary expertise and laboratory capabilities.

METHODS

Ethics approval statement

The Washington University Human Research Protection Office determined that this study (which included fit testing of respirator designs by adult volunteers without collection of personal data) was designated nonhuman subjects research and was exempt from Institutional Review Board oversight (reference ID #202003144).

Overview

Five open-source, improvised respirator designs were selected for testing based on their wide public dissemination (during the early COVID-19 pandemic, March-April 2020) in order to demonstrate testing procedures and identify efficacy and potential limitations (**Figure 2**): a cloth-based respirator ("Sewn Sterilization Wrap")[7], three 3-D printed respirators ("P100 Adaptor"[8], "Self-Moldable 3D Printed"[9], and "Multi-Part 3D Printed"[10]), and one repurposed from medical supplies ("Elastomeric")[11]. These were produced as detailed in **Supplemental Data Document**. A commercial NIOSH-approved N95 respirator (disposable 3M 1860 Health Care Particulate N95 FFR Respirators, 3M, St. Paul, MN) served as control. Experiments were performed in laboratories at our institution. Testing included OSHA-standard quantitative fit testing, filtration testing in an aerosols laboratory, and liquid repellancy testing in a surface chemistry laboratory.

Several of these designs could be fabricated using different filtration media, and we evaluated several candidates that have been proposed for use in these open source designs. Filtration efficiency and liquid repellancy were evaluated for Halyard H600 sterilization wrap (O&M Halyard, Inc., Alpharetta, GA, USA) and Filti™ Face Mask Material (Filti, Inc., Lenexa, KS, USA). In addition, filtration efficiency was also evaluated for a second Halyard sterilization wrap (H500, O&M Halyard, Inc., Alpharetta, GA, USA), material from a commercial N95 respirator (3M™ VFlex™ Healthcare Particulate Respirator and Surgical Mask 1804, 3M, St

Paul, MN), and commercial HVAC material (MERV16 rating), and other configurations of the sterilization wrap materials (two layers of H600, single layers of H600 with stitching).

Patient and public involvement

The authors (including those who originated the study) and fit testing volunteers include intended users (ie. healthcare workers) of the improvised respirator designs studied in this work. No patients were involved in this research.

Quantitative respiratory fit testing

Respirators were quantitatively tested via OSHA 7-minute standardized fit test[17] using a PortaCount Respirator Fit Tester Model 8048 and TSI Model 8026 Particle Generator with TSI FitPro Ultra software. A 4 mm metal grommet was punched through each respirator at a location not in direct contact with skin and connected with 4 mm tubing to the PortaCount device. To facilitate testing of 3D printed respirators, the grommet was inserted through the filter material. To permit passage of a grommet into the filter of the Multi-Part 3D Printed respirator, a soldering iron was used to create a hole in the thermoplastic cap overlying filtration material Three adult volunteers served as standard faces (2 regular, 1 small). The Self-Moldable 3D Printed respirator was molded using hot water as described in design instructions (**Supplemental Data Document**). Each user adjusted respirator placement and strap tightness during real-time fit testing to achieve the best possible fit prior to the 7-minute OSHA standard test. Each design was tested on faces calibrated to small and regular sized surgical N95 filtering facepiece respirators.

Materials testing: Filtration and breathability

Particle filtration performance was evaluated for several materials including commercial filtration materials and fabrics intended for other medical uses. Additional information about testing procedures and a sampling diagram can be found in **Supplemental Data Document, Supplemental Figure 1**. Sample discs of 47 mm were cut directly from the mask or the sourced material sheet and placed in an in-line filter holder during filtration testing (**Supplemental Data Document, Supplemental Figure 2**). A polydisperse NaCl aerosol was produced using a Collison nebulizer, dried to remove water content, and then passed through a charge neutralizer and an electrostatic classifier (TSI Inc., Model 3080 with long differential mobility analyzer column), which selected particles based on their mobility in the electric field with a single-charge diameter setpoint of 300 nm (**Supplemental Data Document** for additional discussion of the particle size). The size-classified aerosol was then charge-neutralized a second time and diluted using HEPA-filtered air to achieve a final particle number concentration in the range of 3000-4000 #/cc. As per our intention to evaluate how these improvised designs compare to the N95 respirators in short supply, this selected size is consistent with similar filtration studies of N95 respirators.[18] Though this diameter is somewhat larger than the size of an isolated SARS-CoV-2 viral particle (approximately 75-105 nm), the virus would most likely be in a larger respiratory particle consisting primarily of water, proteins, salts, and surfactants.[19, 20]

To determine filtration efficiency, particle concentrations upstream and downstream of the filter were measured via continuous condensation particle counter (TSI Inc., Model 3022A). Concentrations were measured in immediate succession to mitigate impact of drift in nebulizer output over time. The NIOSH N95 protocol demands a flow of 85 LPM through the entire respirator, reported to yield a face velocity in the range of 10-13 cm/s for surface areas typical of commercial N95 respirators.[21] We report results here for tests at 7.6 ± 0.1 cm/s, based on the calculated face velocity for the N95 FFR in this study. Particle filtration efficiency values reported here are the average of the three to four different filter punches for the same material. Methods for these calculations are included in **Supplemental Data Document**. The pressure drop across the filter material along with the temperature and relative humidity of the gas passed through the filter were recorded.

Materials testing: Liquid repellency and splatter

Liquid repellency of two of the fabrics used in the alternative respirator designs, Halyard H600 and Filti, were tested through contact angle and fluid penetration measurements. Advancing and receding contact angles were measured by slowly increasing and decreasing the volume of a sessile droplet using a 30 gauge needle and analyzed using ImageJ. [22] Textile liquid absorbency was evaluated via AATCC test method 79-2018.[23] Blood splatter testing followed ASTM F1862 ("Resistance of Medical Face Masks to Penetration by Synthetic Blood") procedures, with the following exceptions: i) Room-temperature whole milk, dyed with red food coloring, replaced the synthetic blood. The surface tension γ_l=49.7 ± 2.0 mN/m was determined using the pendant drop method with a 16 gauge needle, and was independent of the dye concentration.[24] ii) Fabrics were typically not pre-conditioned at 85% relative humidity (RH). Instead, most were stored in a regular laboratory environment (35-55% RH, 22 ± 1°C). iii) Only a limited number of tests (1 to 3 tests) were performed for each impact velocity and fabric. iv) Pressure levels to achieve the required liquid impact velocities (4.5, 5.5, and 6.35 m/s; experimental uncertainty of ± 0.07 m/s) were approximately 34, 50, and 65 kPa, respectively, and were calibrated prior to every test session.

RESULTS

Quantitative respirator fit testing

All but one potential N95 respirator substitute evaluated failed to reach the OSHA half-mask respirator overall fit factor minimum of 100; only the Elastomeric substitute (which uses a commercial HEPA filter for particle filtration mounted to a commercial anesthesia face mask) passed quantitative fit on both small and large face standardized users. Common points of fit failure between respirators were air leak around the nose and difficulty with strap tightening. For 3D printed respirators, users experienced discomfort due to respirator contact at the chin and bridge of the nose. Individual fit factors and points of failure are noted in **Figure 2** and **Supplemental Data Document.** Components of the quantitative fit test for each potential N95 respirator substitutes is noted in **Figure 3.**

The Sewn Sterilization Wrap design failed to reach OSHA specifications (fit factor > 100) for both small and regular respirator size (overall fit factor 20 and 17 respectively. A poor seal was noted around the nose and chin and the rigidness of the straps complicated proper tightening. A fit test was not completed for the P100 filter respirator on small size standardized users due to grossly inadequate seal. Poor fit was additionally noted for regular size standardized users, overall fit factor 17. The Self-Moldable 3D-printed respirator additionally failed to meet OSHA fit standards, overall fit factors 11 and 12 respectively after heat molding. The overall fit factor for the Self-Moldable 3D-printed respirator was not improved by heat molding to users' faces, although it improved subjective user perception of fit with no subjectively noticeable air leak during normal breathing. The Multi-Part 3D printed respirator additionally achieved poor quality seal, overall fit factor 4 and 15 respectively. Users noted circumferential air leak as well as potential air leak surrounding the filter screw threads. The Elastomeric respirator passed fit testing for both small and regular size standardized users, overall fit factor 110 and 108 respectively, however the respirator had inconsistent performance across sections of the fit test and users noted discomfort with the weight of the filter, work of breathing, and strap tightness at which good fit was achieved.

Quantitative fit factors reflect infiltration of particles through both face seal leakage and material penetration, though typical N95 FFRs have such high average filtration efficiency that poor fit is the more likely cause of failed tests (**Supplementary Figure 3**). For improvised designs and materials, particle penetration through the filter media itself could contribute a larger fraction of particles which infiltrate the FFR, as these materials typically have poorer filtration performance. In addition, the 3D-printed designs have a lower filter media surface area, and the resulting higher air face velocities would decrease filtration performance.

Material filtration and air resistance testing

Only the commercial N95 mask material (3M™ VFlex™ Healthcare Particulate Respirator and Surgical Mask 1804, 3M, St Paul, MN) filtered more than 95% of 300 nm particles at a face velocity of 7.6 cm/s (**Figure 4**). In addition, the commercial N95 material had a modest pressure drop of 50 Pa (95% CI: 32 - 69) at this face velocity.

The quality factor (Q) enables evaluation of the trade-off between filter media filtration performance and pressure drop:

$$Q = \ln(1/(1-E)) / \Delta P$$

where E is filtration efficiency, and ΔP is pressure drop. The HVAC (MERV16) and Filti materials had higher quality factors than the sterilization wrap materials, though their performance was more variable (a range of 12% among four punches of Filti and 13% among three punches of the HVAC material). Two sterilization wrap materials (H500 and H600) were tested in a variety of arrangements. As a single layer, H500 and H600 performed similarly, with slightly higher filtration efficiency (70% (95% CI: 67%-72%)) and pressure drop (50 Pa (95% CI: 34 - 66)) for H600. A double layer of H600 (with the flat, less textured sides of the two layers facing inward) improved the filtration efficiency to 89% (95% CI: 86%-91%), though the pressure drop increased. The filtration efficiency measurement for two layers of H600 sterilization wrap was within 5% of that measured by Ou et al.[20], who also evaluated the impact of dry heat, steam, and alcohol decontamination cycles at additional particle diameters.

To evaluate the impact of stitching Halyard material, two lines of stitches (between 6.5 and 7.0 cm total length) were made with a sewing machine in the center of 47 mm discs of H600 material (**Supplemental Document**). The impact of stitching was a decrease in the filtration efficiency from the single layer H600 of 70% (95% CI: 67%-72%) to 65% (95% CI: 60%-71%) for the stitched H600, which also had more variable performance.

A summary of the filtration efficiency and pressure drop measurements are provided in **Supplemental Table 1**.

Breathability of improvised designs

At the test face velocity in this study (7.6 cm/s), none of the materials exceeded the maximum pressure drop across the filter in the NIOSH standard for N95 respirators (343 Pa H_2O during inhalation and 245 Pa during exhalation) to avoid discomfort and detrimental physiological effects.[18, 19] However, the actual face velocity of a respirator undergoing this test (at a flowrate of 85 L/min) would depend on the surface area of filtration material (**Supplemental Figure 4**). For fibrous filters, pressure drop and face velocity are proportional, such that we can use our measurements at a single face velocity to model the pressure drop of each material at the face velocity at which 85 L/min of air would flow through the surface area of each design[25] (**Supplemental Figure 5**).

For all materials, the modeled pressure drop of the Sewn Sterilization Wrap Mask is lower than the maximum standard for inhalation and exhalation. By contrast, only the HVAC material is modeled to meet this breathability standard for any of the 3D printed designs. If the closed area of the mesh grid of the Multi-Part 3D Printed mask is not counted as available filtration surface area, then not even the HVAC material is predicted to meet the NIOSH air resistance standard when used with this design.

Liquid repellency and splatter testing

Test results and optical images of the fabric surfaces (**Figure 5**) shows that both H600 and Filti are repellent towards deionized water and milk (part A: advancing contact angles ≥ 120°), but pose potential liquid penetration points due to millimetric holes in their design. For Halyard, these holes appear sealed, whereas for Filti, the composite fabric consists of a very thin continuous layer sandwiched between two outer layers with the holes in vertical alignment. Both fabrics passed the textile absorbency test with no visible liquid penetration even after multiple minutes. Furthermore, while receding contact angles of milk on both fabrics are zero, milk stains were easily removed by wiping the surface with a wet cloth. When subject to the high-velocity milk jet (part B), however, both fabrics failed splatter testing for a single layer, as confirmed by liquid penetration (part C, bottom image "Layer 1"). When used in a double-layer, H600 was able to prevent liquid break-through for all jet velocities, whereas Filti failed even as a double-layer at higher impingement velocities. Whereas liquid penetration for the top layer happened uniformly at the location of jet impact, penetration for the bottom layer appeared predominantly through the holes in the fabric, and hence was observed more commonly for Filti and not for H600.

DISCUSSION

The COVID-19 pandemic has created significant worldwide shortages in N95 filtering facepiece respirators[26-30] which necessitated development and publication of potential N95 respirator substitutes.[6-11] Given the urgency for these N95 substitutes, safety and efficacy testing prior to their use was limited. Here we presented the results of rigorous, quantitative testing on some of the first open-source alternative N95 substitutes created to address the critical N95 respirator shortage at the start of the COVID-19 pandemic. In this work, a collaborative, interdisciplinary team quantitatively evaluated fit, filtration, and material properties of these N95 open-source substitutes.

The focus of this paper is protocols that can be applied to test the function of improvised masks. When demonstrated on a limited number of volunteers, results revealed that most designs were not sufficiently pliable to match the contours of any of the volunteers, and therefore suggested that these designs might benefit from revision of form or materials that would improve fit prior to mass production. For the one mask that did fit a portion of the volunteers, results emphasize that careful fit testing would be required for each user of the technology. We note that the failure to fit some volunteers is not a failure of the design, in that an improvised design that performed well for individuals with only small and regular faces would still have large benefit in alleviating crisis shortages such as those encountered during the COVID-19 pandemic. In one cohort medium and large sizes were grouped together and only represent 50/229 (21%) of the cohort.[31] Even with appropriate sizes fit testing is further complicated with the shape of users' faces.[32] In addition, with the same protocols required for individuals using a commercial N95 respirator in an occupational setting, fit testing could be used to verify that a particular design had adequate fit for a given individual's face.

Apart from the commercial N95 FFR, only the Elastomeric design passed quantitative fit testing. This design leverages key attributes of its commercial components, including high quality fit of a commercial anesthesia mask and high filtration efficiency of HEPA filter. While we did not directly test the air resistance of a single HEPA filter, the manufacturer's specification (35 mm H2O at 60 L/min) indicates that it exceeds the NIOSH standard (25 mm H2O for exhalation) even at a flowrate (60 L/min) lower than that of the NIOSH test (85 L/min).[33] Thus, a bifurcated adapter for simultaneous use of two filters is recommended for adequate breathability (modeled as 24.8 mm H_2O at 85 L/min). Although the Elastomeric design did pass, its basis off an existing commercial design may limit its implementation for mass production and distribution, as it depends on the availability of the product compared to the manufacturing capabilities of sewn masks or 3D printed designs.

The Sewn Sterilization Wrap Mask was well-tolerated by users, and its larger surface area results in a modeled pressure drop (for all materials) which among the improvised proposed substitutes is most similar to the commercial N95 FFR. Both material filtration testing and quantitative fit testing indicate that its respiratory protection is not equivalent to that of an N95 FFR, though it is likely superior to that of a surgical mask (**Supplementary Figure 3**). Two layers of sterilization wrap also demonstrated fluid resistance in a test with a high velocity jet of milk, though this was not strictly equivalent to the regulatory test method. Filti face mask material would not be an appropriate alternate material for improvised surgical masks or FFRs, unless combined with an additional layer that provided fluid resistance. We note that use in masks is an off-label application of sterilization wrap.

The 3D printed designs yielded 5 of the 6 poorest quantitative fit scores. Quantitative fit testing does not discriminate between particles which infiltrate through leaks in the face seal (or through defects) and particles which penetrate the filtration media itself. The rigidity of the 3D printed designs compromised fit (as well as comfort), and the limited surface area likely exacerbated penetration through the filtration media itself. Though some reports have suggested the use of individual-specific 3D printed masks based on their facial topography, although this may not be practical for a mass production standpoint.[34, 35] At the face velocity calculated for the N95 FFR in this study at the flowrate of a NIOSH particle filtration test, none of the alternate materials filtered more than 95% of particles.[22] Since their lower surface area would result in a higher face velocity in an NIOSH particle filtration test, the 3D printed masks would likely have lower filtration efficiency than reported here for these materials. Only the HVAC material was modeled to have low enough air resistance for the 3D printed designs at these high face velocities, such that we recommend pressure drop measurements of specific filter media proposed for these designs. More specifically, measuring or modeling air resistance at the face velocity which would be encountered in a NIOSH test (at 85 L/min) enables a direct comparison of an improvised design with the N95 standard.

Even without direct filtration testing of full prototypes (which is experimentally more demanding), we demonstrate how quantitative fit testing and material filtration testing can be combined to screen proposed improvised designs together with consideration of air and fluid resistance. These results point to a fundamental need to improve facial fit in future respirator designs, and even more acutely, to an ongoing need during this pandemic for end-users to be equipped and educated for some measure of fit testing. In addition, evaluating designs at the conditions of regulatory test methods (ex. appropriate face velocity for filtration and air resistance) enables direct comparison to the performance expected of a N95 FFR.

There are several limitations to the present study. Our working group identified designs based upon designs in the published literature, designs in the mainstream media, and designs that were proposed to the Washington University hospital system. Although these designs were by no means exhaustive and their selection represented a degree of media bias, they nevertheless represented a sufficiently diverse sampling of improvisation and innovation to illustrate the need to evaluate efficacy and to demonstrate the protocols that are the focus of this paper. Although this study does not evaluate improvised respirator designs as a category (in which case sampling bias would be of concern), and we did not attempt to test all of the large number of potential N95 respirator substitutes. The improvised respirator proposed substitutes were reproduced to the best understanding of posted instructions; however the tested designs may not reflect interval improvements. To demonstrate these protocols, fit testing was carried out with a limited number of individuals who passed fit testing of analogous small and regular size N95 respirators. For designs such as the elastomeric design, which was the only one to passed the fit test for any of the 7 volunteers, additional testing would be warranted for each individual who used this design. Although this limited testing was not designed to develop statistically significant datasets on the proportion of the population that might be able to use each mask design effectively, it did serve to both demonstrate repeatable protocols and to establish limitations of the designs that were not sufficiently pliable to pass fit testing for any of the volunteers.

While filtration testing of material patches at relevant conditions can inform material selection for further development, filtration tests of a mask prototype in its complete form is necessary for evaluation against N95 NIOSH standards, and we continue to develop in-house capacity for these tests. A complication is that the face velocity of a mask depends upon a user's minute ventilation, respiratory rate, inspiratory time, and the mask surface area, complicating comparison of masks and protocol standardization. Whole milk was used to test the splatter resistance of the fabrics, as artificial blood was not readily accessible. While the measured surface tension is within the range of surface tension of typical body fluids and blood at body temperature [24, 36] it is slightly higher than that of synthetic blood as prescribed by F1862, which could result in favorable test results, as fluids with lower surface tension are known to wet surfaces more easily.[37]

The potential N95 respirator substitutes tested here were attempts to meet immediate needs of the COVID-19 pandemic frontline. However, our data indicates the majority of these proposed substitutes do not have equivalent respiratory protection and breathability to a N95 FFR. The majority of masks tested revealed inherent design issues such as inadequate filtration capabilities of the base materials and poor ergonomic facial fit to a variety of facial shapes and sizes. Our experience has highlighted the importance for institutions to be equipped and educated to perform appropriate qualitative and quantitative testing prior to novel mask implementation. This study reveals that rapid creation of an improvised respirator with N95 performance utilizing readily available materials and simple manufacturing methods is extremely challenging, and consequently there is an emergent need for in-house testing platforms to better understand the degree to which protection is being provided. Healthcare professionals requiring this a high level of respiratory protection should be cautious of claims associated with improvised respirators when suggested as N95 replacements without quantitative evaluation.

CONTRIBUTORSHIP STATEMENT

Author contributions:

Concept and experimental design: DHB, AJD, BMK, PBW, JMM, BAB, JTB, NHS, PKW, PB, RLA, GMG, BJW, KWM
Experimental studies: DHB, AJD, BMK, PBW, JMM, ARS, MRS, BAB, JAM, CG, JH, BK, UJ, SC, DIAD, BM, CM, JTB, NHS, PKW, BJW, KWM
Data collection: DHB, AJD, BMK, PBW, JMM, ARS, MRS, BAB, JAM, CG, JH, BK, UJ, SC, DIAD, BM, JTB, NHS, PKW, BJW, KWM
First manuscript draft: DHB, AJD, BMK, PBW, JMM, ARS, MRS, BAB, JAM, CG, JH, BK, SS, SYL, SC, DIAD, NHS, RLA, GMG, BJW, KWM
Critical revision: DHB, AJD, BMK, PBW, JMM, ARS, BAB, BK, JTB, PKW NHS, RLA, GMG, BJW, KWM
Approval of final manuscript: All authors

DATA SHARING STATEMENT

Data not presented in the present manuscript may be provided by the corresponding author upon a reasonable request.

REFERENCES

1. Rational Use of Personal Protective Equipment for Coronavirus Disease 2019 (COVID-19) – Interim Guidance February 27, 2020. World Health Organization Website.

Available at: https://apps.who.int/iris/bitstream/handle/10665/331215/WHO-2019-nCov-IPCPPE_use-2020.1-eng.pdf Accessed on April 13, 2021.

2. "Protecting Healthcare Workers During the COVID-19 Pandemic: A Survey of Infection Preventionists March 27, 2020." Association for Professionals in Infection Control and Epidemiology. Available at: https://apic.org/wp-content/uploads/2020/03/Protecting-Healthcare-Workers-Survey_Report_3_26_20_Final.pdf. April 13, 2021.
3. Provenzano D, Rao YJ, Mitic K, Obaid SN et al. Rapid Prototyping of Reusable 3D-Printed N95 Equivalent Respirators at the George Washington University. *Biomedical and Chemical Engineering* 2020; 2020030444. Ahead of print. doi:10.20944/preprints202003.0444.v1
4. Liu DCY, Koo TH, Wong JKK, et al. Adapting re-usable elastomeric respirators to utilise anaesthesia circuit filters using a 3D-printed adaptor - a potential alternative to address N95 shortages during the COVID-19 pandemic. *Anaesthesia*. 2020;75(8):1022–1027.
5. Elkington P, Dickinson A, Mavrogordato M, et al. A Personal Respirator Specification for Health-care Workers Treating COVID-19 *(PeRSo)*. Ahead of print. doi:10.31224/osf.io/rvcs3.
6. COVID-19 Supply Chain Response Collection. NIH 3D Print Exchange Website. Available at: https://3dprint.nih.gov/collections/covid-19-response/search Accessed on April 13, 2021.
7. Mask Alternative. University of Florida College of Medicine Department of Anesthesiology Website. Available at: https://anest.ufl.edu/clinical-divisions/mask-alternative/#prototype2 Accessed on April 13, 2021.

8. 3D Printed N95 Replacement Mask. Barrow Neurological Institute Website. Available at: https://www.barrowneuro.org/get-to-know-barrow/barrow-innovation-center-2/3d-printed-n95-mask/. Accessed on April 13, 2021.

9. The Montana Mask. Make the Masks Website. Available at: https://www.makethemasks.com/. Accessed on October 2, 2020. Content no longer available at given website April 13, 2021; archived page available at request.

10. The "MalaMask" Project (N95 Alternative Filter). River City Labs Website. Available at: https://wiki.rivercitylabs.space/covid-19/3d-printed-masks. Accessed on April 13, 2021.

11. Surgical Innovation Fellowship. Boston Children's Hospital Website. Available at: http://www.childrenshospital.org/research/departments-divisions-programs/departments/surgery/surgical-innovation-fellowship. Accessed on April 13, 2021.

12. Radonovich LJ, Jr, Simberkoff MS, Bessesen MT, et al. N95 Respirators vs Medical Masks for Preventing Influenza Among Health Care Personnel: A Randomized Clinical Trial. *JAMA* 2019;322(9):824-33.

13. Janssen L, Ettinger H, Graham S, Shaffer R, Zhuang Z. The use of respirators to reduce inhalation of airborne biological agents. *J Occup Environ Hyg*. 2013;10:D97-D103.

14. N95 Decontamination & Reuse Method Decision Matrix, N95DECON Website. Available at: https://static1.squarespace.com/static/5e8126f89327941b9453eeef/t/5ffe0c426639ea757c0ee5e7/1610484802173/20200816_N95_Decontamination_Reuse_Comparison_Matrix.pdf. Accessed on April 13, 2021.

15. Viscusi DJ, Bergman MS, Eimer BC, Shaffer RE. Evaluation of five decontamination methods for filtering facepiece respirators. Ann Occup Hyg. 2009;53:815–827.

16. Boškoski I, Gallo C, Wallace MB, Costamagna G. COVID-19 pandemic and personal protective equipment shortage: protective efficacy comparing masks and scientific methods for respirator reuse. Gastrointest Endosc. 2020;92:519–523.

17. Appendix A to §1910.134—Fit Testing Procedures (Mandatory). United States Department of Labor Website. Available at: https://www.osha.gov/laws-regs/regulations/standardnumber/1910/1910.134AppA. Accessed on April 13, 2021.

18. Balazy A, Toivola M, Reponen T, Podgorski A, Zimmer A, Grinshpun SA. Manikin-Based Performance Evaluation of N95 Filtering-Facepiece Respirators Challenged with Nanoparticles. *Ann Occup Hyg.* 2005;50:259-69.

19. Martines RB, Ritter JM, Matkovic E, et al. Pathology and Pathogenesis of SARS-CoV-2 Associated with Fatal Coronavirus Disease, United States. Emerging Infect Dis. 2020;26(9).

20. Johnson, G. R.; Morawska, L.; Ristovski, Z. D.; Hargreaves, M.; Mengersen, K.; Chao, C. Y. H.; Wan, M. P.; Li, Y.; Xie, X.; Katoshevski, D.; et al. Modality of Human Expired Aerosol Size Distributions. *J. Aerosol Sci.* **2011**, *42* (12), 839–851.

21. Airflow resistance test. Cornell Law School Legal Information Institute. Available at https://www.law.cornell.edu/cfr/text/42/84.172 Accessed on April 13, 2021.

22. Chen V, Long K, Woodburn EV. When weighing universal precautions, filtration efficiency is not universal. *J Hosp Infect*. 2020. Ahead of print. DOI: 10.1016/j.jhin.2020.04.032.

23. Ou Q, Pei C, Chan Kim S, Abell E, Pui DYH. Evaluation of decontamination methods for commercial and alternative respirator and mask materials – view from filtration aspect. J Aerosol Sci. 2020;150:105609.

24. Stalder AF, Kulik G, Sage D, Barbieri L, Hoffmann P. A snake-based approach to accurate determination of both contact points and contact angles. *Colloid Surface A.* 2006;286:92-103.

25. Hinds, W. C. *Aerosol Technology*, 2nd ed.; Wiley: Hoboken, 1999.

26. van Doremalen N, Bushmaker T, Morris DH, et al. Aerosol and Surface Stability of SARS-CoV-2 as Compared with SAS-CoV-1. *N Engl J Med* 2020;382:1564-7.

27. Bauchner H, Fontanarosa PB, Livingston EH. Conserving Supply of Personal Protective Equipment—A Call for Ideas. *JAMA* 2020;323(19):1911.

28. Wong SC-Y, Kwong RT-S, Wu TC, et al. Risk of nosocomial transmission of coronavirus disease 2019: an experience in a general ward setting in Hong Kong. *J Hospl Infect* 2020;105(2):119–127.

29. Lu J, Gu J, Li K, et al. COVID-19 Outbreak Associated with Air Conditioning in Restaurant, Guangzhou, China, 2020. *Emerg Infect Dis.* 2020;26.

30. Santarpia JL, Rivera DN, Herrera V, et al. Transmission Potential of SARS-CoV-2 in Viral Shedding Observed at the University of Nebraska Medical Center. *Infectious Diseases (except HIV/AIDS)* 2020. Ahead of print. doi:10.1101/2020.03.23.20039446.

31. Bergman M, Zhuang Z, Brochu E, Palmiero A. Fit Assessment of N95 Filtering-Facepiece Respirators in the U.S. Centers for Disease Control and Prevention Strategic National Stockpile. J Int Soc Respir Prot. 2015;32:50–64.

32. ASTM F3407-20, Standard Test Method for Respirator Fit Capability for Negative-Pressure Half- Facepiece Particulate Respirators. ASTM International, West Conshohocken, PA, 2020. Available at: http://www.astm.org/cgi-bin/resolver.cgi?F3407. Accessed April 13, 2021.

33. Ultipor® 25 Anesthesia Filter with Monitoring Port . Available at: https://shop.pall.com/us/en/products/zidBB25AB?CategoryName=&CatalogID=&tracking=searchterm. Accessed April 13, 2021.

34. Swennen GRJ, Pottel L, Haers PE. Custom-made 3D-printed face masks in case of pandemic crisis situations with a lack of commercially available FFP2/3 masks. Int J Oral Maxillofac Surg. 2020;49(5):673–677.

35. Scott AR, Hu J, Gan C, Morris JA, Meacham KW, Ballard DH. Safety concerns for facial topography customized 3D-printed N95 filtering face-piece respirator produced for the COVID-19 pandemic: initial step is respiratory fit testing. Int J Oral Maxillofac Surg. 2020. Ahead of print. DOI: 10.1016/j.ijom.2020.08.017.

36. AATCC TM79-2010e2(2018)e, AATCC Website. Available at: https://members.aatcc.org/store/tm79/499/. Accessed on April 13, 2021.

37. Daerr A, Mogne A. Pendent_Drop: An ImageJ Plugin to Measure the Surface Tension from an Image of a Pendent Drop. *J Open Res Softw*. 2016; 4: e3.

Figure Legends

Figure 1. Overview of essential surgical N95 attributes.

Figure 2. The 5 designs are displayed with an image of them on a user in the second column, and the filter material used in the second column. The last two columns present the respirators stratified by standardized face size of the user. Radial bar plots display Overall Fit Factor from the OSHA 7-minute standardized fit test for each design as well as the 3M N95 for regular and small size standardized users. Green bars represent passing scores, 100 or greater, while red bars indicate failing scores. Areas noted by users to leak air were highlighted.

Figure 3. Fit scores across the 6 scored OSHA fit test sections are displayed for each respirator. An overall fit factor of 100 is required to pass testing, however a respirator need not pass all fit testing segments as the total fit score is a weighted average of all segments.

Figure 4. (a) Quality factor, (b) filtration efficiency (primary y-axis, red), and pressure drop (secondary y-axis, blue) observed for materials tested with an air flow face velocity of 7.6 ± 0.1 cm/s and 300 nm challenge NaCl particles. Error bars for filtration efficiency and pressure drop are 95% confidence intervals for mean values (represented as horizontal lines). 95% filtration efficiency is marked as a dashed red line.

Figure 5. Fabric characterization: Wettability and splatter testing. **A**. Wetting: Optical images of the two tested fabrics (Halyard and Filti), along with images of milk droplets with advancing contact angles of 120° and 127°, respective. Visible holes pin the liquid (receding contact angles:

0°) and are a possible weak point for liquid penetration. **B**. Repellency: Splatter testing, *i.e.*, resistance to high-velocity liquid jet penetration (test liquid: whole milk at 4.5, 5.5, and 6.35 m/s), for single (left half-circle) and double (right half-circle) layers of Halyard and Filti fabrics. Red indicates repellency failure, *i.e.*, penetration of liquid through the fabric layer(s). Green indicates a passed test, if the majority of sampled fabrics did not show milk break-through. **C**. Multilayer: Optical image of the front (top) and inter-layer (bottom) surfaces after liquid jet impingement. Milk (dyed with red food color) penetrated the first layer and deposited on the underlying layer, but did not break through the second layer.

Supplemental Figure 1. Flow diagram of the aerosol filtration testing station.

Supplemental Figure 2. 47 mm discs were cut from H600 sterilization wrap fabric sheets (Halyard Health, Alpharetta, GA) and stitched with two straight lines using a sewing machine. The total length of stitching on each of the three filters was 6.7, 6.5, and 7.0 cm.

Supplemental Figure 3. Lines represent combinations of material filtration efficiency performance (%) and leakage (ie. around the face seal or through defects; % of flowrate) which result in a given fit factor.

Supplemental Figure 4. Face velocity of 85 L/min as a function of filtration surface area.

Supplemental Figure 5. For several materials, pressure drop is modeled as a function of face velocity. Vertical lines represent the characteristic face velocity for 85 L/min flowrate through the filtration area of the improvised designs.

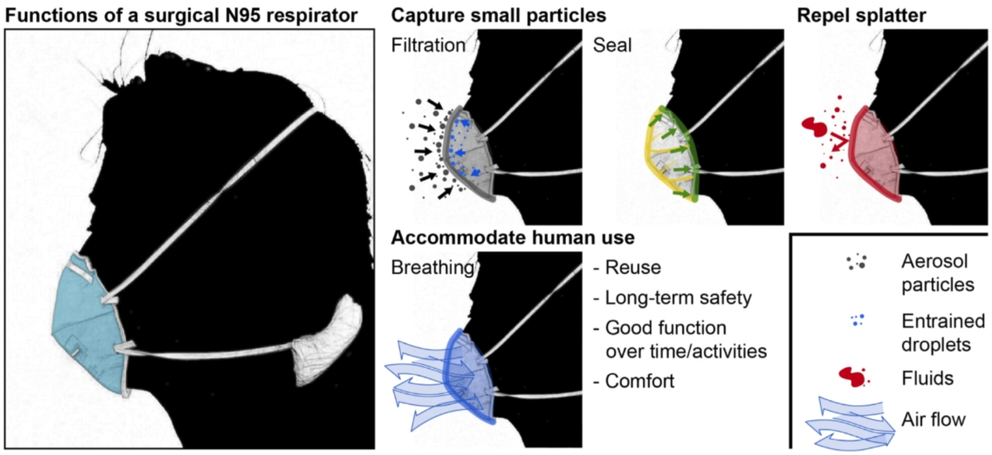

Figure 1. Overview of essential surgical N95 attributes.

260x121mm (300 x 300 DPI)

Figure 2. The 5 designs are displayed with an image of them on a user in the second column, and the filter material used in the second column. The last two columns present the respirators stratified by standardized face size of the user. Radial bar plots display Overall Fit Factor from the OSHA 7-minute standardized fit test for each design as well as the 3M N95 for regular and small size standardized users. Green bars represent passing scores, 100 or greater, while red bars indicate failing scores. Areas noted by users to leak air were highlighted.

160x146mm (300 x 300 DPI)

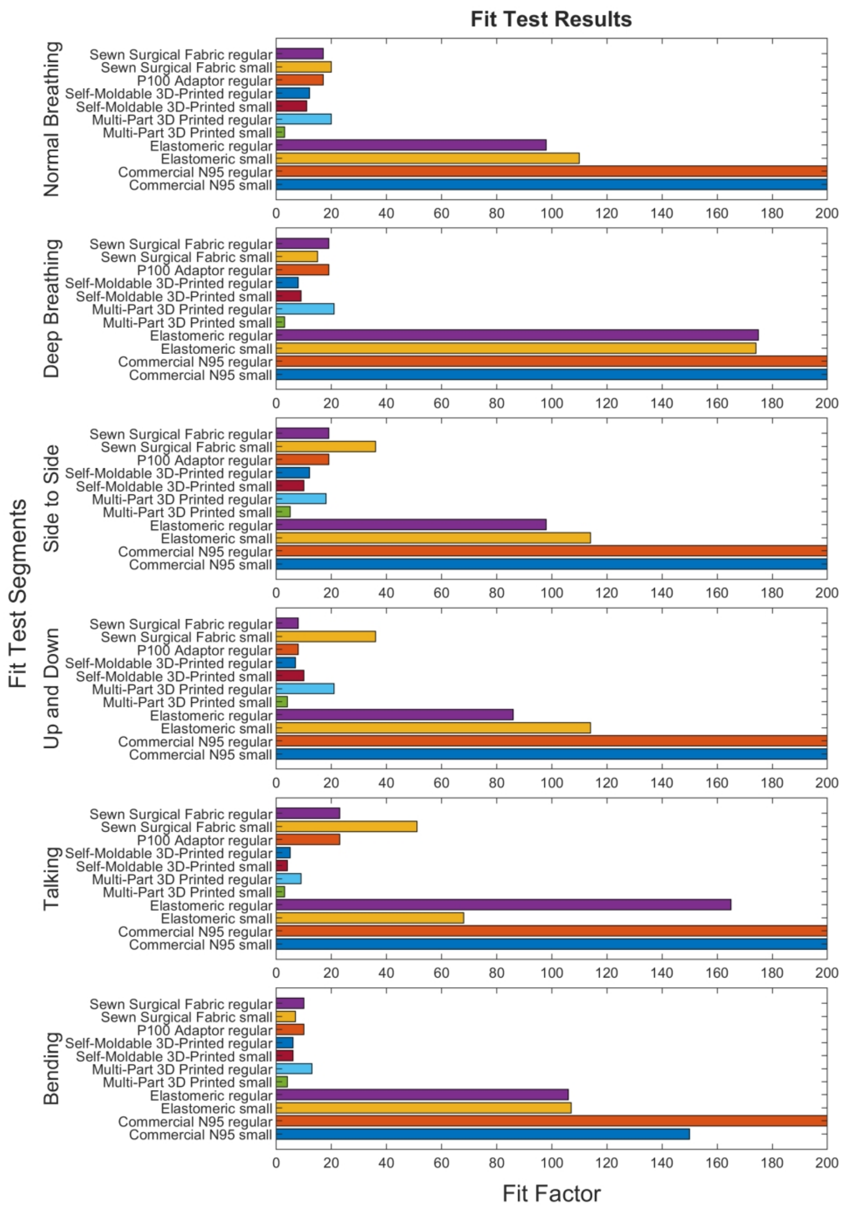

Figure 3. Fit scores across the 6 scored OSHA fit test sections are displayed for each respirator. An overall fit factor of 100 is required to pass testing, however a respirator need not pass all fit testing segments as the total fit score is a weighted average of all segments.

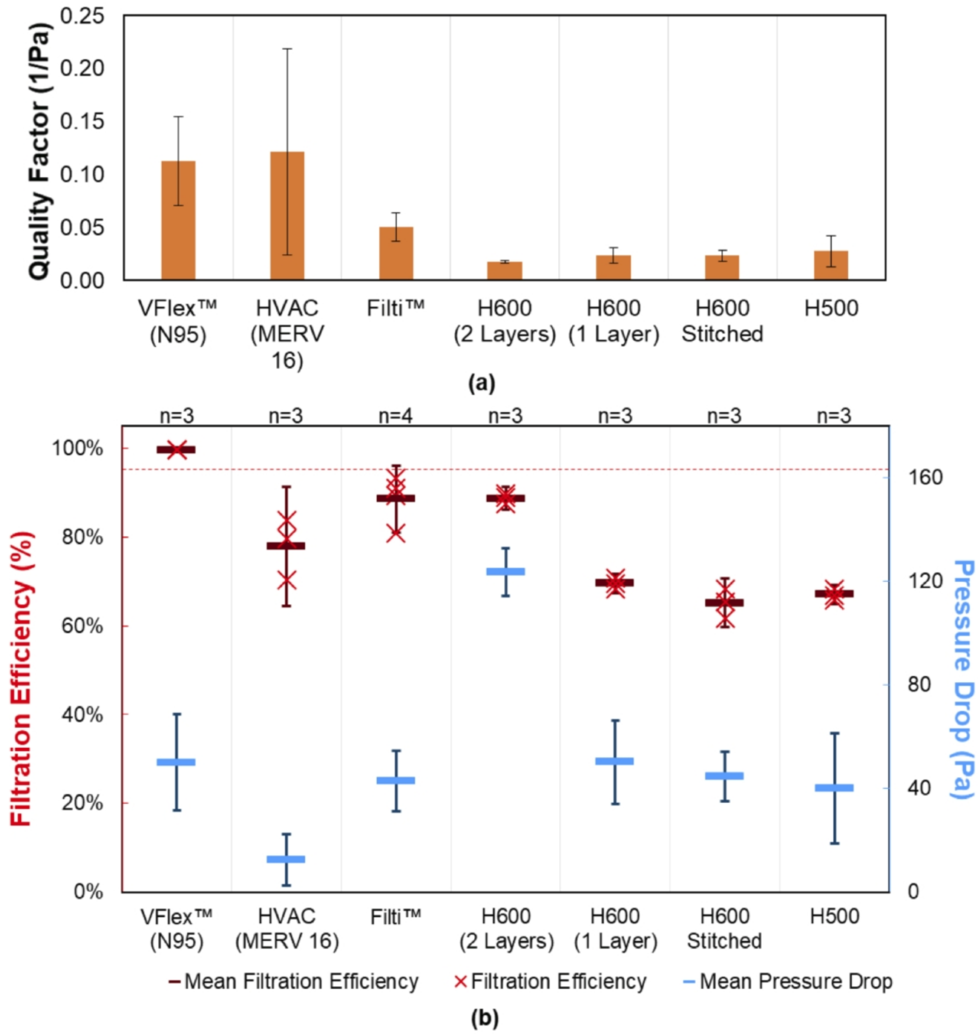

Figure 4. (a) Quality factor, (b) filtration efficiency (primary y-axis, red), and pressure drop (secondary y-axis, blue) observed for materials tested with an air flow face velocity of 7.6 ± 0.1 cm/s and 300 nm challenge NaCl particles. Error bars are 95% confidence intervals for mean values. 95% filtration efficiency is marked as a dashed red line.

205x220mm (600 x 600 DPI)

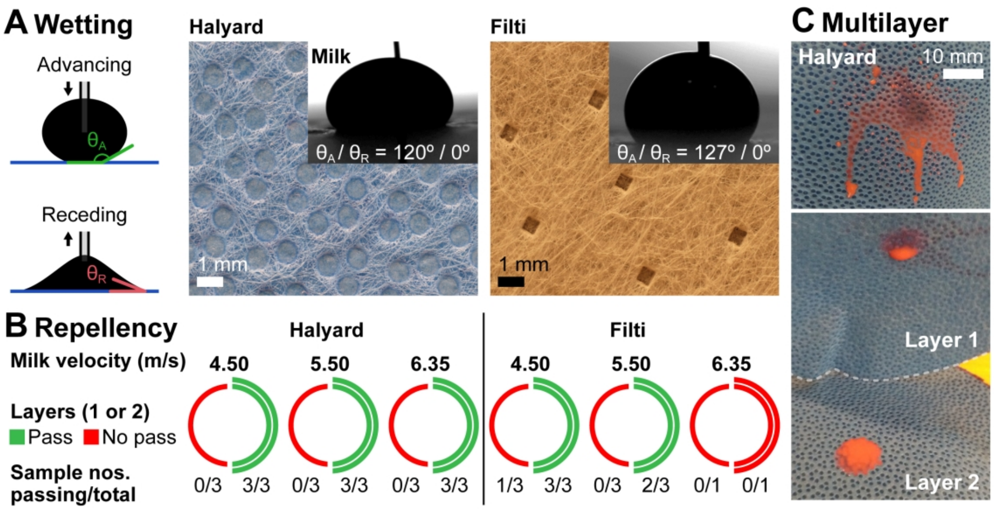

Figure 5. Fabric characterization: Wettability and splatter testing. A. Wetting: Optical images of the two tested fabrics (Halyard and Filti), along with images of milk droplets with advancing contact angles of 120° and 127°, respective. Visible holes pin the liquid (receding contact angles: 0°) and are a possible weak point for liquid penetration. B. Repellency: Splatter testing, i.e., resistance to high-velocity liquid jet penetration (test liquid: whole milk at 4.5, 5.5, and 6.35 m/s), for single (left half-circle) and double (right half-circle) layers of Halyard and Filti fabrics. Red indicates repellency failure, i.e., penetration of liquid through the fabric layer(s). Green indicates a passed test, if the majority of sampled fabrics did not show milk break-through. C. Multilayer: Optical image of the front (top) and inter-layer (bottom) surfaces after liquid jet impingement. Milk (dyed with red food color) penetrated the first layer and deposited on the underlying layer, but did not break through the second layer.

Supplemental Figure Document

Supplemental Figure 1.

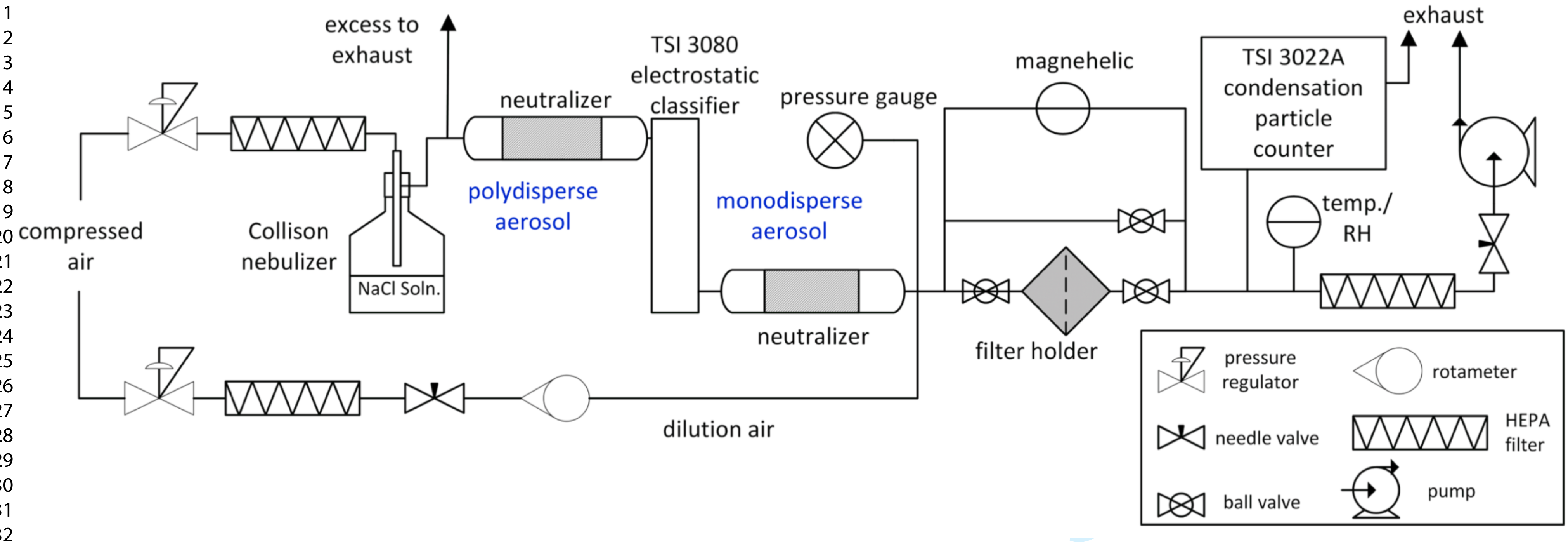

Supplemental Figure 1. Flow diagram of the aerosol filtration testing station.

Supplemental Figure 2.

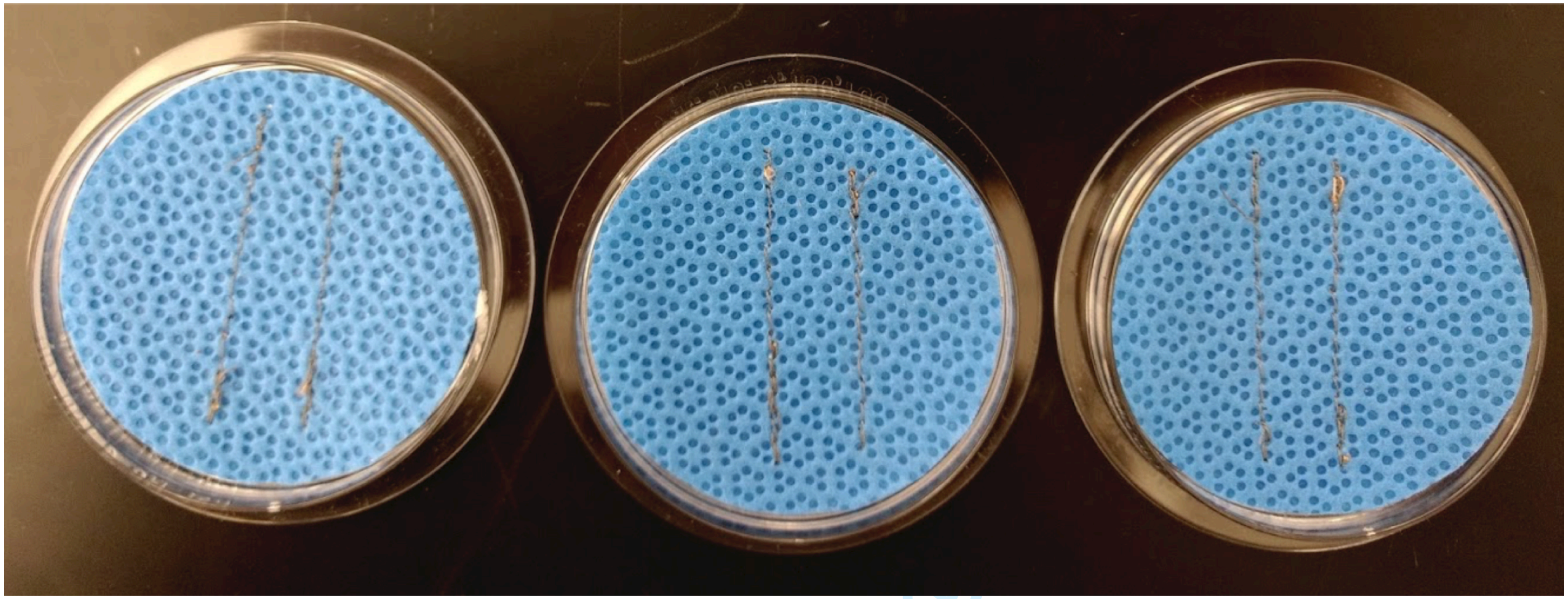

Supplemental Figure 2. 47 mm discs were cut from H600 sterilization wrap fabric sheets (Halyard Health, Alpharetta, GA) and stitched with two straight lines using a sewing machine. The total length of stitching on each of the three filters was 6.7, 6.5, and 7.0 cm.

Supplemental Figure 3.

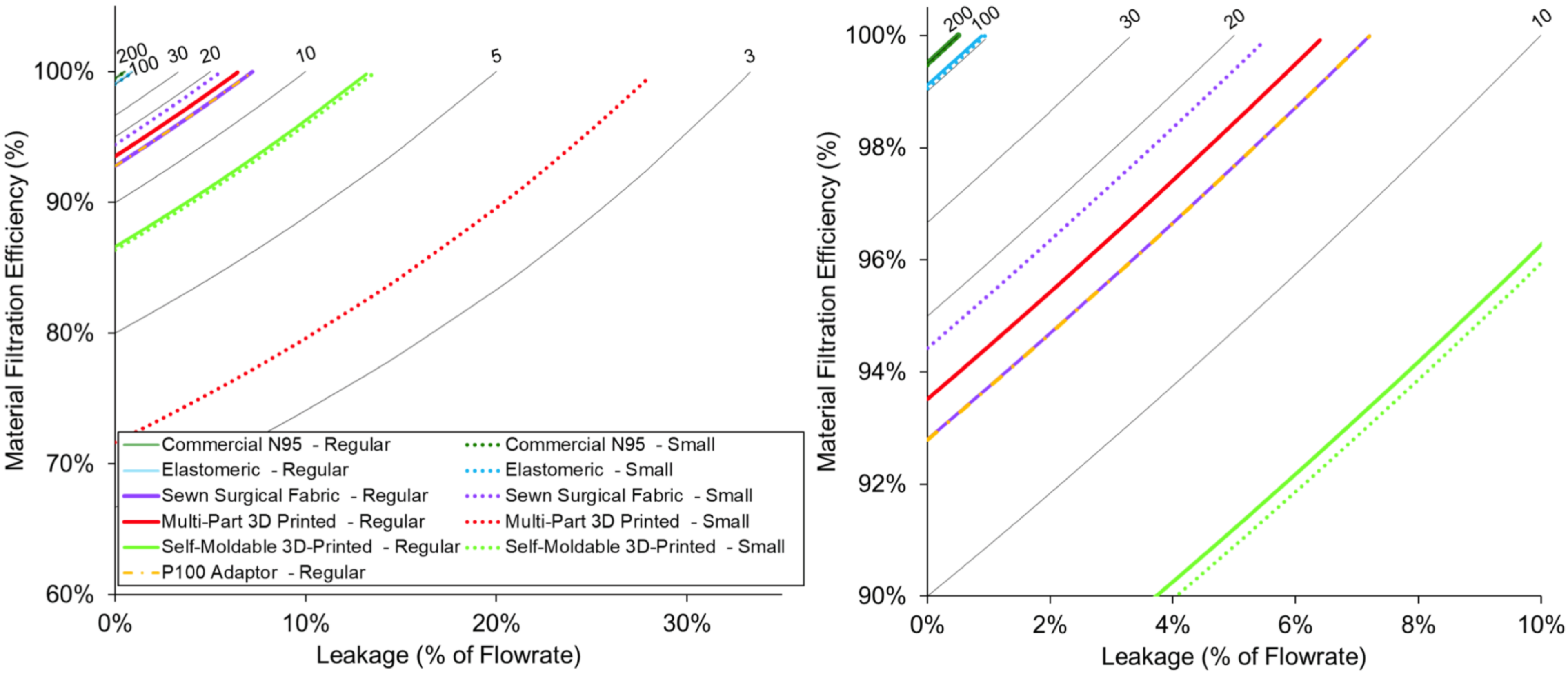

Supplemental Figure 3. Lines represent combinations of material filtration efficiency performance (%) and leakage (ie. around the face seal or through defects; % of flowrate) which result in a given fit factor.

Supplemental Figure 4.

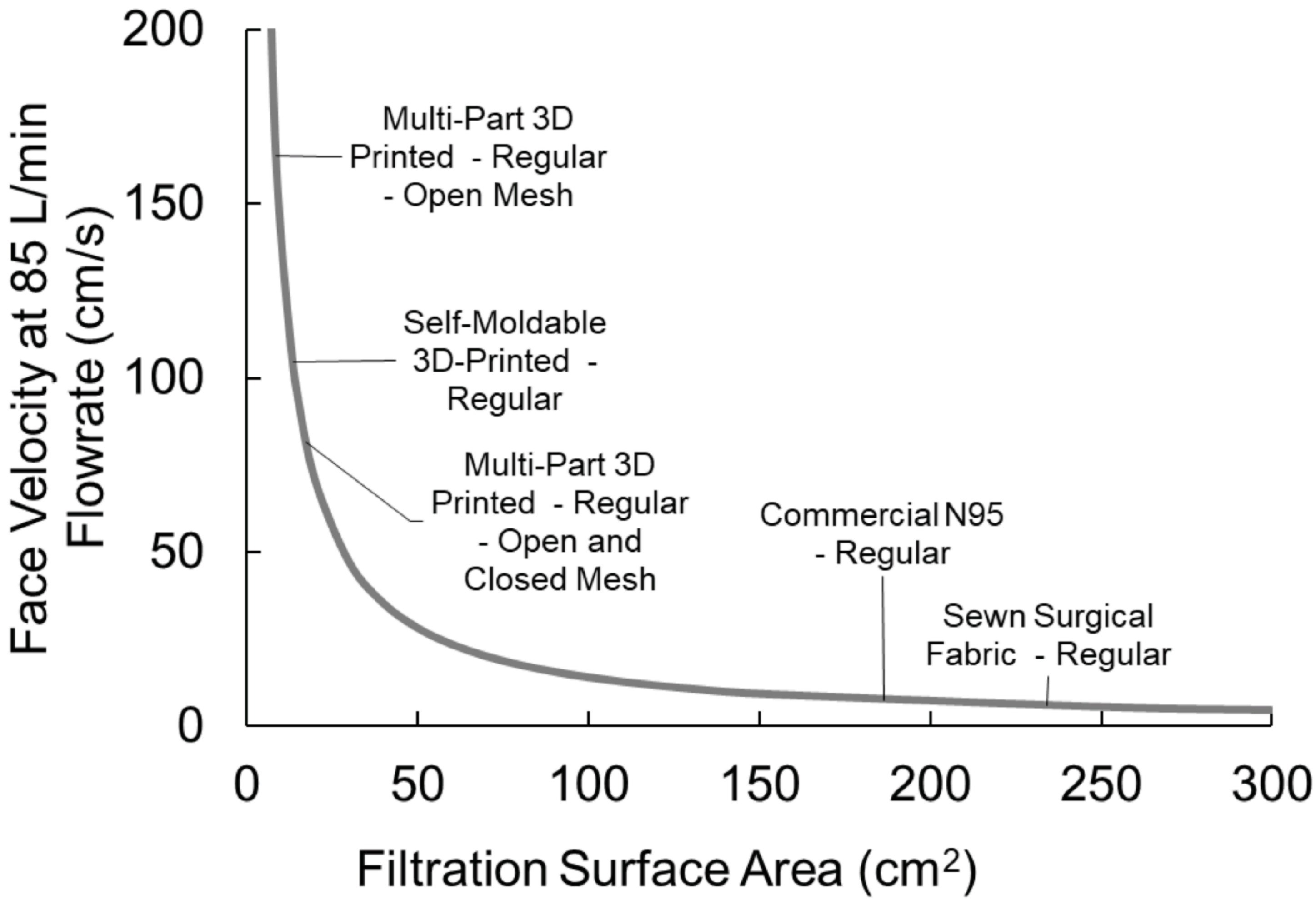

Supplemental Figure 4. Face velocity of 85 L/min as a function of filtration surface area.

Supplemental Figure 5.

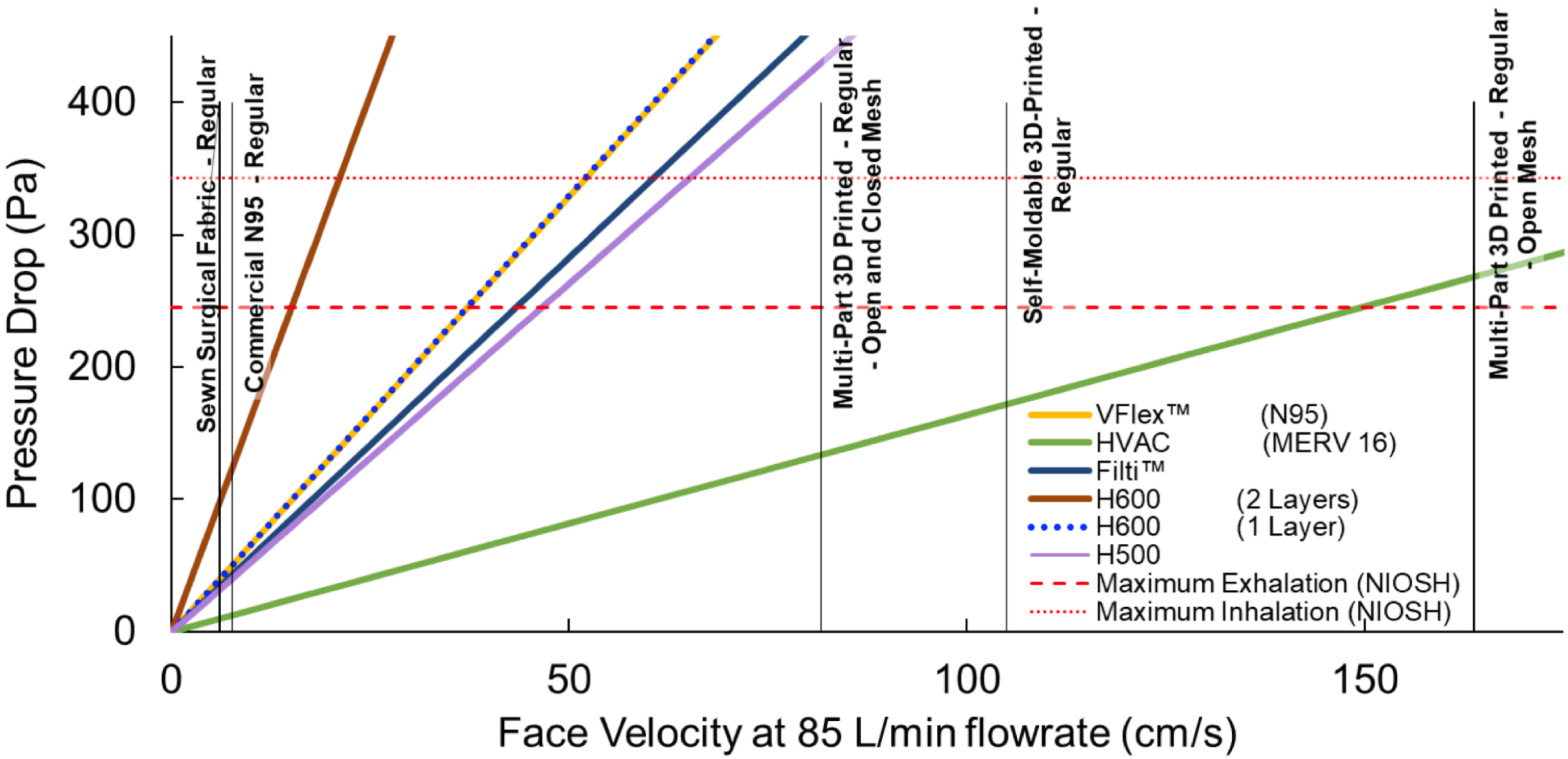

Supplemental Figure 5. For several materials, pressure drop is modeled as a function of face velocity. Vertical lines represent the characteristic face velocity for 85 L/min flowrate through the filtration area of the improvised designs.

Supplementary Mask Fabrication Methods

For 3D printed respirator designs, a number of different 3D printers and materials were used depending on availability. For sewn respirators, traditional sewing machines were used by experienced sewers. In all cases, fabrication followed the process defined in the online instructions. Detailed fabrication procedures for the five designs, named as follows in the main text: P100 Adaptor, Multi-part 3D Printed Mask, Sewn Sterilization Wrap, Commercial Elastomeric Respirator, Self-Moldable 3D Print. All links were retrieved on May 1, 2020.

Sewn Sterilization Wrap

The Florida mask pattern and instructions were downloaded from the University of Florida Department of Anesthesiology website.[1] Two layers of Halyard 600 sterilization wrap (Halyard, Alpharetta, GA) was cut according to the pattern downloaded and printed from the website. The masks were assembled with a Janome Memory Craft (Janome, Tokyo, Japan) home sewing machine according to the detailed instructions provided. Spandex elastic 3/8 inch (0.952 cm) wide was attached at the specified locations.

P100 Adaptor

Manufacture of the "P100 Adaptor" mask followed open source instructions created at the Barrow Innovation Center (Phoenix, AZ).[2] Mask parts were produced by fused deposition modeling 3D printing and silicone casting for fit. Parts were printed in PLA (grey stock 1.75 mm from Prusa) with 20% infill and a shell thickness of 4 perimeters using a .4 mm nozzle on a Prusa i3 MK3s. The print layer height was .2 mm thickness. Print temperature was 200°C with a print bed temperature of 70°C. A soldering iron was used to melt perforations in 3D printed mask perimeter. A mold was created from a production staff member's face, encasing the printed shell of the mask with clay. This clay mold was then removed, and a silicone seal was cast. Assembly of the mask required manually clearing the holes in the plastic shell and trimming clearance for elastic head straps to pass silicone seal. An O-ring seal was applied prior to attachment of a p100 filter.

Specifications were followed as described in the document from the Barrow Innovation Center, with a few exceptions as follows. The silicone mold as described was observed to be too thick to obtain a completed seal, so the edge of mold was sculpted back for a better fit. Moreover, the seal as described did not stay adhered to the mask shell on first casting and had to be glued after removal from mold. Although the end user would ideally be present for mask production to ensure personalized fit, this was not possible in our fabrication process, and masks were molded to the face of a production staff member.

Self-Moldable 3D Print

"Self-Moldable 3D Print" masks designs were obtained from open source instructions provided by Make the Masks.[3] 3D printer files were formatted in Simplify3D (Simplify3D, Cincinnati, OH) for use on the Fusion3 F410 (Fusion 3D, Greensboro, NC) single filament printer with a 0.4 mm diameter print head and standard 1.75 mm PLA. Head temperature was set at 240°C. Test prints priors were conducted at infills of 10%, 15%, 20% and 25% with aspect ratios of 90%, 95%, and 100%, corresponding to small, medium, and large face sizes. These test prints were sanded, cleaned, and test fit to gauge pliability under heat molding as outlined by the designers. Lower infills yielded more pliable masks but ran the risk of allowing perforations in the print layers that compromised the integrity of the mask. After these preliminary test prints, prototype samples were printed with a print head temperature of 230°C, with extrusion and print speeds lowered to 90%, and monitored for the duration of the print to ensure quality of layer adhesion at an infill of 15% in aspect ratios of 90% and 100%. Masks were individually molded to user faces using a hot water dip and adequate molding was established by forcibly exhaling against a blocked filter to identify points of air leak prior to quantitative testing.

Multi-part 3D Printed Mask

Manufacture of the "Multi-part 3D Printed Mask" closely followed open source instruction provided online by River City Labs.[4] Parts were printed in PLA (grey stock 1.75 mm from Prusa, Prague, Czech Republic) with 20% infill and a shell thickness of 3 perimeters using a .4 mm nozzle on a Prusa i3 MK3s. The print layer height was .2 mm thickness. Print temperature was 200°C with a print bed temperature of 70°C. Notably, a deviation in the printing process from the instructions was use of PLA rather than Polyethylene Terephthalate Glycol-modified (PETG) due to supply availability. For filtration material, Merv 13 (AAF International, Doraville, GA) was substituted for Merv 16 due to local supply limitations. After 3-D printing from the file provided and testing the seal mold, adjustments to the external geometry were needed to enable fitting. To address this, an alternative seal mold external geometry was developed to allow for better closure, but this still failed to yield a perfect seal. Seals did not self-retain on the contoured mask shell due to low elasticity of the seals, requiring gluing to the shell edge. Additionally, extensive hand finishing was not performed on exterior parts or on threads of articulating parts due to increasing thread tolerance and worsening seal.

Commercial Elastomeric Respirator

Instruction for fabrication were obtained from open source documents provided on the Boston Children's Hospital Website.[5] The "Commercial Elastomeric Respirator" was fabricated by mounting a Ultipor 25 Ventilator Inline Bacterial/Viral Filter (Pall Corporation, Westborough, MA) on an anesthesia face mask with one end open to the environment. A face piece-filter adapter with integrated sampling port was 3D printed of polylactic acid (PLA) using fused deposition modeling (Prusament PLA; Prusa i3 MK3S, Prusa Research, Prague, CZ). The sampling port was tapped to receive a 1/4 inch-28 compression fitting to seal around fluorinated ethylene propylene (FEP) tubing with an outer diameter of 1/8 in (3.12 mm). The mask was then secured using elastic straps attached to the 4-pronged ring surrounding the inflow and outflow tract.

<u>Supplementary Splatter testing Methods</u>

For splatter testing, a Nordson EFD ValveMate 8000 (Nordson Corporation, Westlake, OH) with a 741V pneumatic valve generated the liquid jet. Fabrics, either as a single or a double layer, were secured using a 1/16 inch (0.159 cm) rubber cuff over a polyethylene terephthalate (PET) 3D printed backing form with the standard-specified dimensions. A 0.25 inch (0.635 cm) centering hole, drilled into an acrylic sheet, was placed approximately 0.5 inches (1.27 cm) from the respirator surface, and the valve with an 18 gauge needle was placed at a distance of 12 inches (30.5 cm). After impingement, fabrics were visually inspected for liquid penetration.

<u>Supplementary Filtration Methods</u>

A flow diagram of the particle testing station is provided in Figure S1. Sample discs of 47 mm were extracted directly from the mask or the sourced material sheet and placed in a stainless steel in-line filter holder (Pall #2220, Pall Corporation, Westborough, MA), which exposed a circular area of 35 mm diameter during filtration testing. A polydisperse NaCl aerosol was produced from a 1.0 %wt. NaCl solution in DI water using a Collison Nebulizer (CH Technologies) and an in-line custom diffusion dryer, with a pressure of 8 psig (55.2 kPa) and a flow rate of 6 liters per minute (LPM). The aerosol was then passed through an electrostatic classifier (TSI Inc., Model 3080, Shoreview, MN, with long differential mobility analyzer (DMA) column, operated with a sheath flowrate of 5 LPM and an aerosol flow rate of 1.46 LPM ± 0.04, which was set by controlling the pressure at the exit of the DMA by continually adjusting the needle valve to vacuum) to select particles based on mobility in the electric field with a peak mobility size of 300 nm mean diameter. Electric mobility is proportional to the ratio of particle charge and aerodynamic diameter (equivalent to diameter for spherical particles), such that for a given diameter setpoint, a set of particles of increasing diameter and discrete charge (ie. +1, +2, etc.) will be selected by the DMA. Since the mode of the nebulizer size distribution is less than the 300 nm setpoint and since the aerosol is neutralized prior to the DMA, the singly charged particles (with 300 nm diameter mode) will predominate. After the classifier, the aerosol was neutralized a second time by flowing through a tube with two imbedded Po-210 strips (NRD Staticmaster 2U500, Grand Island, NY) and then diluted with HEPA-filtered house air. In the case of samples at 4.38±0.05 LPM (corresponding to 7.6±0.1 cm/s face velocity to the exposed filter area), an additional 2.92 LPM of using HEPA-filtered house air was added to achieve a final particle number concentration in the range of 3000 - 4000 particles per cubic centimeter. To determine the filtration efficiency, the concentrations of particles upstream and downstream of the filter were measured using a continuous condensation particle counter (TSI Inc., Model 3022A). Upstream and downstream particle concentrations were measured in immediate succession to mitigate impact of drift in nebulizer output over time. The flow through the filter material was varied to achieve a range of face velocities. The pressure drop across the filter material was measured with a magnehelic differential pressure gauge (Dwyer, Michigan City, IN) and the temperature and relative humidity of the gas passed through the filter was measured with an industrial probe (Dwyer HHT Series). Relative humidity and temperature were not actively controlled and were within the range of 8 and 21 % relative humidity and 19.4 and 21.1°C for the results presented here.

Methods of calculation

Particle filtration efficiency for a single punch was calculated from the unfiltered and filtered particle concentrations ($C_{Unfiltered}$ and $C_{Filtered}$ respectively):

$$(Filtration\ Efficiency) = 1 - \frac{C_{Filtered}}{C_{Unfiltered}}.$$

$C_{Unfiltered}$ and $C_{Filtered}$ were calculated as the mean of replicate measurements through the bypass line and filter respectively for the same punch:

$$C = \frac{1}{J}\sum_{j=1}^{J} \bar{x}_j$$

where $\bar{x}_j$ is the j^{th} replicate measurement (of a total of J) for a given condition (filtered or unfiltered) and is calculated from the mean concentration (#/cc) recorded by the condensation particle counter (CPC) (for at least 30 s at 1 s time resolution):

$$\bar{x}_j = \frac{1}{n_{CPC}} \sum_{i=1}^{n_{CPC}} x_i$$

where x_i is the i^{th} raw concentration datum (of a total of n_{CPC} data) recorded by the CPC. $C_{Unfiltered}$ was also corrected for particle penentration (99.4% ± 2.4) through the empty filter holder relative to the bypass line:

$$C_{Unfiltered} = (99.4\%) \cdot \frac{1}{J} \sum_{j=1}^{J} \bar{x}_j$$

The uncertainty in filtration efficiency is the combined uncertainty of the two measurements as well as the uncertainty in the measurement of particle penetration through the empty filter holder:

$$S_{Efficiency} = (1 - Filtration\ Efficiency) \sqrt{\left(\frac{2.4\%}{99.4\%}\right)^2 + \left(\frac{S_{Unfiltered}}{C_{Unfiltered}}\right)^2 + \left(\frac{S_{Filtered}}{C_{Filtered}}\right)^2}.$$

The uncertainty of the unfiltered or filtered particle concentration ($S_{unfiltered}, S_{filtered}$) for a punch was calculated as the combined error from the maximum relative CPC variability (S_{CPC}) observed for that condition and punch and the variability between replicate measurements of the filtered or unfiltered particle concentrations (S_{Punch}):

$$S = \sqrt{{S_{CPC}}^2 + {S_{Punch}}^2}$$

$$S_{CPC} = max\left(\frac{s_{CPC,j}}{\bar{x}_j \sqrt{n_{CPC}}}\right) \times C$$

where n_{CPC} is the number of CPC measurements and $s_{CPC,j}$ is the standard deviation of the raw CPC data:

$$s_{CPC,j} = \sqrt{\frac{\sum_{i=1}^{n_{CPC}}(x_i - \bar{x}_j)^2}{n_{CPC} - 1}}$$

Given the evolving and urgent demand for this data, the number of replicates of measurements of $C_{Unfiltered}$ and $C_{Filtered}$ for a single punch ($n_{condition,unfiltered}$ and $n_{condition,filtered}$) varied from one unfiltered and one filtered measurement to three unfiltered and two filtered measurements (with the mean of each condition used to calculate filtration efficiency). These replicate measurements were always performed in immediate succession to mitigate any long-term nebulizer output drift. In cases where the unfiltered or filtered particle concentration $\bar{x}_j$ was measured multiple times for a single punch (with the mean value C used to calculate the particle capture efficiency), S_{Punch} was calculated as the standard error of the mean of these replicate measurements:

$$S_{Punch} = \frac{\sqrt{\frac{\sum(y_j - \bar{y})^2}{n_{condition} - 1}}}{\sqrt{n_{condition}}}$$

where $n_{condition}$ is the number of replicate measurements for that condition and punch.

As discussed previously, for several punches, only a single unfiltered or filtered measurement were taken. Since a standard error cannot be computed for a single replicate, we estimated S_{Punch} using the standard error of an estimate calculated for the regression of repeat measurements (*n*=16 for unfiltered measurements, *n*=13 for filtered measurements) versus time in a separate test with the same sample flowrate and diameter setpoint. This approach yields estimates of $\frac{S_{Punch,filtered}}{C}$ of 1.43% and $\frac{S_{Punch,unfiltered}}{C}$ of 0.93%.

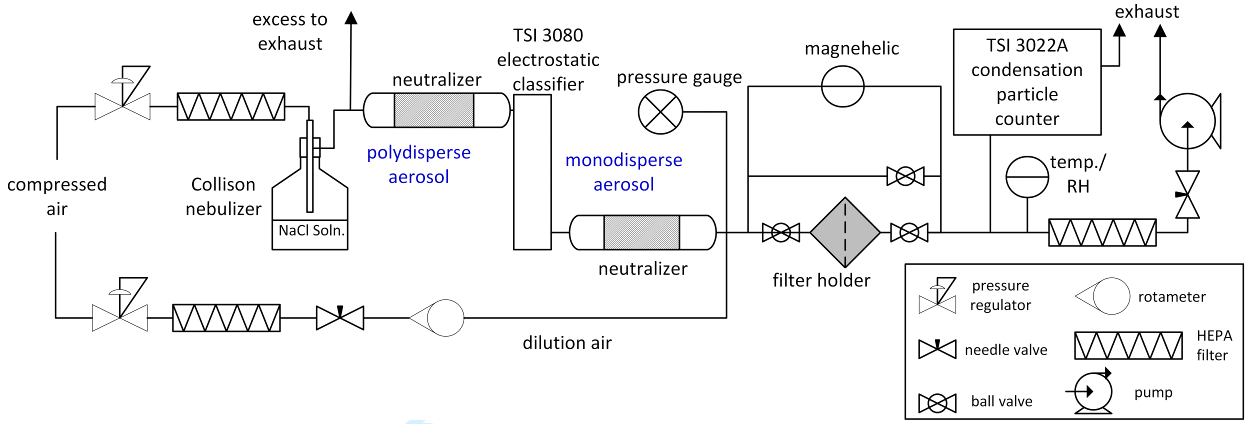

Supplemental Figure 1. Flow diagram of the aerosol filtration testing station.

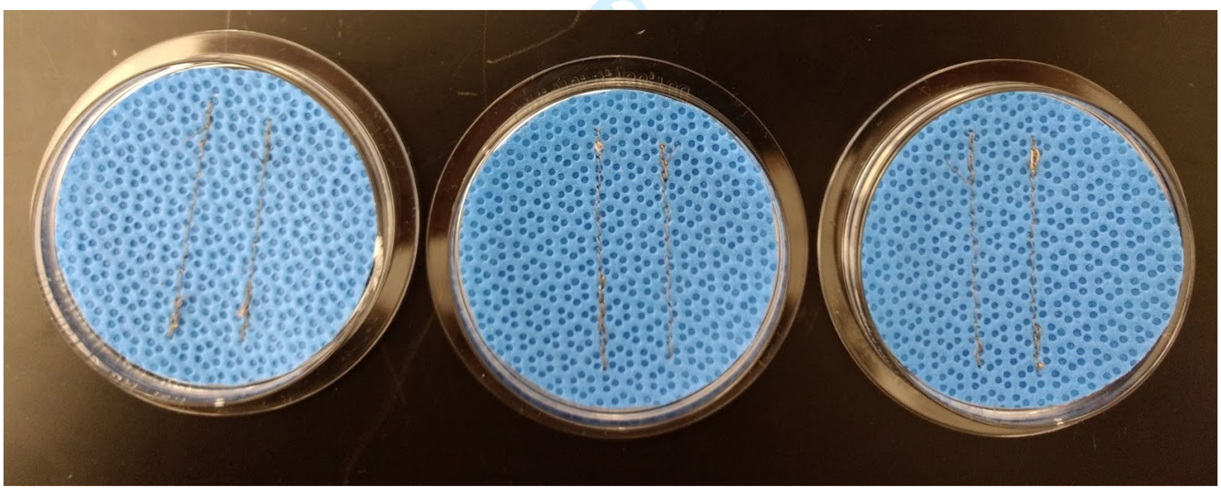

Supplemental Figure 2. 47 mm discs were cut from H600 sterilization wrap fabric sheets (Halyard Health, Alpharetta, GA) and stitched with two straight lines using a sewing machine. The total length of stitching on each of the three filters was 6.7, 6.5, and 7.0 cm.

Supplemental Table 1. Filtration efficiencies and mean pressure drop of filtration efficiencies.

	Filtration Efficiencies of Replicate Punches (%) (Standard Uncertainty)				Mean Filtration Efficiency (%)	Mean Pressure Drop (Pa)
	Punch #1	Punch #2	Punch #3	Punch #4	(95% Confidence Interval)	(95% Confidence Interval)
VFlex ™ (N95)	99.659% (99.649% - 99.669%)	99.67% (99.65% - 99.69%)	99.600% (99.590% - 99.610%)		99.64% (99.55% - 99.74%)	50 (32 - 69)
HVAC (MERV 16)	83.8% (83.3% - 84.3%)	79.7% (79.2% - 80.3%)	70.3% (69.5% - 71.1%)		78% (65% - 91%)	12 (3 - 22)
Filti™	81% (80% - 82%)	90.9% (90.7% - 91.2%)	93.2% (93.0% - 93.4%)	89.3% (89.0% - 89.6%)	89% (81% - 96%)	43 (31 - 55)
H600 (2 Layers)	87.5% (87.1% - 87.8%)	89.0% (88.7% - 89.3%)	89.7% (89.4% - 89.9%)		89% (86% - 91%)	124 (114 - 133)
H600 (1 Layer)	69.6% (68.8% - 70.4%)	70.7% (69.8% - 71.6%)	68.4% (67.6% - 69.2%)		70% (67% - 72%)	50 (34 - 66)
H600 Stitched	62% (60% - 63%)	65% (64% - 67%)	68.3% (67.4% - 69.2%)		65% (60% - 71%)	45 (35 - 54)
H500	66.9% (66.0% - 67.7%)	65.9% (64.9% - 66.9%)	68.4% (67.6% - 69.2%)		67% (65% - 69%)	40 (19 - 61)

Replicate intervals represent standard uncertainty, and mean intervals represent 95% confidence intervals.

<u>Supplementary Discussion of Individual Discussion of Respirators</u>

Sewn Sterilization Wrap

The sewn sterilization wrap was well tolerated by participants who noted its breathability and easily understandable speech. Nevertheless, the respirator presented a poor seal with multiple points of air leak including the nose, chin and cheeks. The respirator surface area is small compared to many currently marketed duckbill respirators and these leaks may be improved by extending the material outward across the cheeks and further below the jawline. Additionally, users noted difficulty with tightening the respirator straps due to lack of elasticity, with additionally restricted head motion when the lower strap was tightened with the head in a neutral position and the participants were instructed to look upward. Circumferential seal can be potentially improved with more elastic straps to provide additional tension to the sides of the respirator.

P100 Adaptor

Due to fabrication limitations users were not present for silicone molding and fitting and consequently the respirator was unable to be tested on a small sized user due to gross mismatch in size and circumferential lack of seal. Users noted easy breathability, but the hard-plastic design contacting the chin created discomfort while talking and acted as a lever during upward head motion reducing perceived seal. The strength of the straps was also insufficient to support the weight of the respirator with the attached filter and caused pulling away from the face during downward movements. While ideally respirators would have been molded individually to the end users this highlights a crucial challenge in widespread implementation.

Self-Moldable 3D Print

The Self-Moldable 3D Print respirator was well tolerated with easy breathability and speech comprehension. Users performed fit testing prior to individualized heat molding (described in supplementary methods) and noted that perceived air leaks were resolved with molding, however fit factor was not improved. Without fit testing this may lead to a false assurance of respirator fit and underscores the importance of proper fit testing. Additionally, users found the heat molding process to be difficult and cumbersome and a potential challenge to widespread implementation.

Multi-part 3D-Printed Mask

The multi-part 3D-printed respirator was poorly tolerated by users due to discomfort at the nose bridge and cheek bones from the hard-plastic fit as well as highly muffled and near incomprehensible speech. The multi-part design introduced several potential locations for air leak, most notably the lack of an O-ring rubber seal between the threads of the 3D respirator shell and filter housing. On forceful exhalation users noted potential air leak around the filter. Material and fabrication constraints are discussed in the supplemental methods and represent challenges with wide implementation of the potential N-95 respirator substitutes .

Commercial Elastomeric Respirator

The Commercial Elastomeric Respirator was poorly tolerated by users, both commented on discomfort at the bridge of the nose which may be attributable to greater tension on the upper strap necessary to achieve good fit. This was partially relieved by increasing inflation of the respirator, however fully inflating the respirator for user comfort compromised fit during real-time testing. Additionally, users noted difficulty with talking due to tension placed on the jaw. Speech was highly muffled and difficult to understand. Furthermore, the weight of the filter caused subjective difficulty with fit during head motion and may explain the inconsistency in fit across fit test segments. Additionally, users commented on the difficulty of adjusting respirator tightness due to the high elasticity of the straps, which was necessary to counteract the high weight of the respirator. Iterations of this respirator with a single filter were found to be significantly more difficult to breathe through compared to those with a bifurcated adaptor that allowed for attachment of two separate filters.

REFERENCES

7. Mask Alternative. University of Florida College of Medicine Department of Anesthesiology Website. Available at: https://anest.ufl.edu/clinical-divisions/mask-alternative/#prototype2 Accessed on April 13, 2021.

8. 3D Printed N95 Replacement Mask. Barrow Neurological Institute Website. Available at: https://www.barrowneuro.org/get-to-know-barrow/barrow-innovation-center-2/3d-printed-n95-mask/. Accessed on April 13, 2021.

9. The Montana Mask. Make the Masks Website. Available at: https://www.makethemasks.com/. Accessed on October 2, 2020. Content no longer available at given website April 13, 2021; archived page available at request.

10. The "MalaMask" Project (N95 Alternative Filter). River City Labs Website. Available at: https://wiki.rivercitylabs.space/covid-19/3d-printed-masks. Accessed on April 13, 2021.

11. Surgical Innovation Fellowship. Boston Children's Hospital Website. Available at: http://www.childrenshospital.org/research/departments-divisions-programs/departments/surgery/surgical-innovation-fellowship. Accessed on April 13, 2021.